

Portland State University

PDXScholar

Environmental Science and Management
Faculty Publications and Presentations

Environmental Science and Management

2016

Madagascar's Mangroves: Quantifying Nation-Wide and Ecosystem Specific Dynamics, and Detailed Contemporary Mapping of Distinct Ecosystems

Trevor G. Jones

Portland State University

Leah Glass

Blue Ventures Conservation

Samir Gandhi

Blue Ventures Conservation

Lalao Ravaoarinorotsihoarana

Blue Ventures Conservation

Aude Carro

Blue Ventures Conservation

Follow this and additional works at: https://pdxscholar.library.pdx.edu/esm_fac



next page for additional authors

Part of the Biodiversity Commons, and the Environmental Monitoring Commons

Let us know how access to this document benefits you.

Citation Details

Jones, T., Glass, L., Gandhi, S., Ravaoarinorotsihoarana, L., Carro, A., Benson, L., ... Cripps, G. (2016). Madagascar's Mangroves: Quantifying Nation-Wide and Ecosystem Specific Dynamics, and Detailed Contemporary Mapping of Distinct Ecosystems. *Remote Sensing*, 8(2), 106. <http://doi.org/10.3390/rs8020106>

This Article is brought to you for free and open access. It has been accepted for inclusion in Environmental Science and Management Faculty Publications and Presentations by an authorized administrator of PDXScholar. Please contact us if we can make this document more accessible: pdxscholar@pdx.edu.

Authors

Trevor G. Jones, Leah Glass, Samir Gandhi, Lalao Ravaoarinosihoarana, Aude Carro, Lisa Benson, Harifidy Rakoto Ratsimba, Chandra Giri, Dannick Randriamanatena, and Garth Cripps

Article

Madagascar's Mangroves: Quantifying Nation-Wide and Ecosystem Specific Dynamics, and Detailed Contemporary Mapping of Distinct Ecosystems

Trevor G. Jones^{1,2,*}, Leah Glass¹, Samir Gandhi¹, Lalao Ravaoarinosihoarana¹, Aude Carro¹, Lisa Benson¹, Harifidy Rakoto Ratsimba³, Chandra Giri⁴, Dannick Randriamanatena⁵ and Garth Cripps¹

¹ Blue Ventures Conservation, Villa Bella Fiharena, Rue Gambetta, Lot 259, Toliara, Madagascar; leah@blueventures.org (L.G.); srgandhi87@gmail.com (S.G.); lalao@blueventures.org (L.R.); aude@blueventures.org (A.C.); lisa.benson@blueventures.org (L.B.); garth@blueventures.org (G.C.)

² Dynamic Ecosystems and Landscapes Lab, Department of Environmental Science and Management, Portland State University, Portland, OR 97201, USA

³ Department of Forestry, PO Box 175, University of Antananarivo, Antananarivo 101, Madagascar; rharifidy@yahoo.fr

⁴ United States Geological Survey, Earth Resources Observation and Science Center, Duke University, Durham, NC 27708, USA; cgiri@usgs.gov

⁵ WWF Madagascar West Indian Ocean Programme Office, Antsakaviro, B.P. 738, Antananarivo 101, Madagascar; drandriamanatena@wwf.mg

* Correspondence: trevor@blueventures.org

Academic Editors: Randolph H. Wynne and Prasad S. Thenkabail

Received: 31 August 2015; Accepted: 8 January 2016; Published: 30 January 2016

Abstract: Mangrove ecosystems help mitigate climate change, are highly biodiverse, and provide critical goods and services to coastal communities. Despite their importance, anthropogenic activities are rapidly degrading and deforesting mangroves world-wide. Madagascar contains 2% of the world's mangroves, many of which have undergone or are starting to exhibit signs of widespread degradation and deforestation. Remotely sensed data can be used to quantify mangrove loss and characterize remaining distributions, providing detailed, accurate, timely and updateable information. We use USGS maps produced from Landsat data to calculate nation-wide dynamics for Madagascar's mangroves from 1990 to 2010, and examine change more closely by partitioning the national distribution in to primary (*i.e.*, >1000 ha) ecosystems; with focus on four Areas of Interest (AOIs): Ambaro-Ambanja Bays (AAB), Mahajamba Bay (MHJ), Tsiribihina Manombolo Delta (TMD) and Bay des Assassins (BdA). Results indicate a nation-wide net-loss of 21% (*i.e.*, 57,359 ha) from 1990 to 2010, with dynamics varying considerably among primary mangrove ecosystems. Given the limitations of national-level maps for certain localized applications (*e.g.*, carbon stock inventories), building on two previous studies for AAB and MHJ, we employ Landsat data to produce detailed, contemporary mangrove maps for TMD and BdA. These contemporary, AOI-specific maps provide improved detail and accuracy over the USGS national-level maps, and are being applied to conservation and restoration initiatives through the Blue Ventures' Blue Forests programme and WWF Madagascar West Indian Ocean Programme Office's work in the region.

Keywords: Madagascar; mangrove; Landsat; dynamics; coastal

1. Introduction

Found in over 120 countries and territories between 30°N and 30°S latitude, mangrove ecosystems support high floral and faunal biodiversity and provide a diverse range of goods (*e.g.*, food, fuel,

building materials) and services (e.g., water filtration; storm protection) to coastal populations. Furthermore, a growing number of studies report that mangroves possess similar or greater above- and exceptionally larger below-ground carbon stocks as compared with their terrestrial peers [1–25], meaning that intact mangrove ecosystems contribute to global climate change mitigation through sequestering significant amounts of CO₂. Despite their tremendous and diverse value, throughout the world mangrove ecosystems are rapidly being degraded, deforested and converted for other uses. Over the past several decades, annual global mangrove loss is estimated at 1%–2%, exceeding rates in many inland tropical forests [6,26–30]. The primary drivers of loss include conversion for agri- and aquaculture, coastal development, over-extraction of woody materials, and the ripple effects of upstream terrestrial agriculture and deforestation (*i.e.*, erosion, sedimentation and siltation) [31–40]. While anthropogenic activities are the primary drivers of loss, natural phenomena such as tropical storms and rising ocean temperatures and sea-levels also play a significant role; the impacts of which are expected to continue to increase based on current climate change projections [6,11,30,31,37,40–45]. Many of the world's enduring mangrove ecosystems have already been degraded, and may functionally collapse within this century without intervention [27,46,47].

To quantify dynamics and initiate effective management and decision-making, contemporary information on the extent and status of mangrove ecosystems is required. Remotely sensed data can be employed to map and monitor mangrove ecosystems, providing managers and decision makers with detailed, accurate, timely and updateable information [15,48]. In particular, the Landsat archive, which extends back >40 years, is well tested for identifying and quantifying mangrove distribution and dynamics, and for mapping and monitoring specific mangrove ecosystems at the level of thematic detail required for management strategies [25,49–65]. As described in [66], there is a growing need to use remotely sensed data such as Landsat to monitor shifts in stable states in coastal wetlands, such as mangroves. New techniques which go beyond single-date mapping and multi-date change detection are needed to create evolutionary models of mangroves; pushing the boundaries of Landsat-like remotely sensed data [66]. Along these lines, a recent study in the Mekong delta by [67] demonstrates how to study the spatial and temporal evolution of mangroves using a time series of Landsat data augmented by Shuttle Radar Topography Mission (SRTM) data. Factoring in the need for and benefit of monitoring shifts in stable states, detailed, contemporary single-date maps are still required for many management tasks and are unavailable for much of the world's mangrove ecosystems [25,61].

The island nation of Madagascar contains extensive mangrove ecosystems, which as of 2005 totaled approximately 280,000 hectares (ha); Africa's fourth largest amount and 2% of the global distribution [10,57,68,69]. Many of Madagascar's mangrove ecosystems have undergone or are starting to show signs of wide-spread degradation and deforestation. To date, numerous studies have employed remotely sensed data to produce single- or multi-date nation-wide mangrove maps (*i.e.*, [68–72]). However, national-level maps, while critical for country-wide overviews, do not provide the thematic detail required for many localized (e.g., ecosystem-specific) applications. Prior to 2010, localized mapping was undertaken for several specific mangrove ecosystems (*i.e.*, Bombetoka Bay, Betsiboka Estuary, Mahajamba Bay (MHJ), and Mangoky Delta) (*i.e.*, [73–77]). However, these maps are either out-of-date or lack the thematic detail required for certain management initiatives (e.g., carbon stock inventories); and for many of Madagascar's mangrove ecosystems, are simply non-existent.

Here, we inventory and compare existing national-level mangrove maps for Madagascar. Using the most comprehensive and contemporary available data, we quantify nation-wide mangrove dynamics from 1990 to 2010. To use these data to examine dynamics at a finer scale, we partition Madagascar's mangroves in to non-contiguous, primary (*i.e.*, >1000 ha) mangrove ecosystems; with focus on four distinct mangrove ecosystems representing areas of interest (AOIs): Ambaro-Ambanja Bays (AAB), MHJ, Tsiribihina Manambolo Delta (TMD) and Baie des Assassins (BdA). Given the limitations of national-level maps for certain localized applications, and the limitations of existing and/or lack of ecosystem-specific maps for AOIs, we build on two previous studies for AAB and MHJ [25,61] and employ Landsat data to produce detailed, contemporary, maps of TMD and BdA.

The applications of existing (AAB; MHJ) and new (TMD; BdA) AOI-specific maps to mangrove conservation initiatives through Blue Ventures' Blue Forests programme are discussed.

2. Experimental Section

2.1. Study Area

The study area includes the entire distribution of Madagascar's mangroves (Figure 1). Madagascar's ~5000 km coastline is one of the most extensive shallow marine areas in the Western Indian Ocean (WIO), wherein mangrove ecosystems are located almost entirely along the west coast. While not as species-rich as other regions, at least eight true mangrove species occur, supporting unique flora and fauna, much of which is currently endangered or at-risk [12,68].

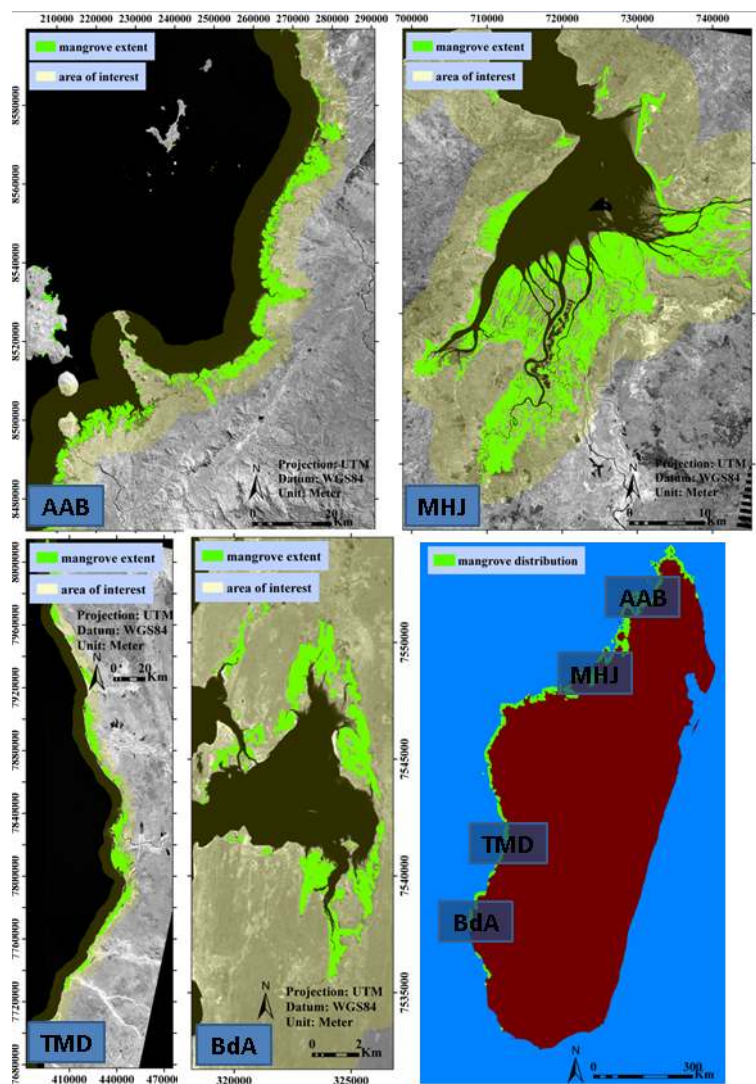


Figure 1. The study area includes the entire distribution of Madagascar's mangroves (shown in green, *circa* 2010, bottom right) (data obtained with permission from Giri [69]). The combined marine and terrestrial extent within 7 km from the coast in four primary mangrove ecosystems (*i.e.*, Ambaro-Ambanja Bays (AAB), Mahajamba Bay (MHJ), Tsiribihina-Manambolo Delta (TMD) and the Baie des Assassins (BdA)) represent four specific areas of interest (AOIs). The location of each AOI is shown in the country-wide inset (bottom right). Mangrove extent (*circa* 2010) within each AOI is shown in green (data obtained with permission from Giri [69]).

Madagascar's mangrove ecosystems are governed by a complex legal framework involving forestry, land planning, fisheries and environmental laws [78–85]. The most relevant texts regarding mangrove management and use are found in the forestry and environmental sectors. Under forestry laws, mangroves are within the public domain of the state, but local communities can be granted user rights for their domestic use of related resources, including timber [78,80,82]. Under environmental laws, mangroves fall within the sensitive area category, in which an environmental impact assessment is compulsory prior to any type of investment, and where commercial timber extraction has been forbidden since 2000 [79,81]. More recently, in 2014 a Decree was issued by the Government of Madagascar to ban the extraction, transportation, stocking and sale of timber specifically in mangrove ecosystems [85]. In practice, the Forestry Administration continues to grant communities user rights on mangrove timber, despite the two-above mentioned bans. Local management rights can be established through either Protected Areas or Natural Resource Management Transfer regulations; though this process is complex, expensive and time consuming. Regardless of management rights, comprehensive and effective management, which impedes mangrove degradation and loss, is lacking for almost all mangrove ecosystems in Madagascar. Due to the lack of governance, an increasing demand in fuel-wood and timber, as well as the expansion of agricultural land, the pressure on mangrove ecosystems from anthropogenic activities continues to rise [25]. If degradation and conversion continue unimpeded, biodiversity will be imperiled, greenhouse gas emissions will increase, and many important services provided to coastal communities will be seriously compromised [86].

Owing to the lack of effective mangrove management in Madagascar and local people's high dependence on the numerous goods and services mangroves provide, the marine conservation NGO Blue Ventures (www.blueventures.org) initiated its Blue Forests programme in 2011, to work with coastal communities, partner NGOs, Malagasy and foreign Universities, and government bodies at all levels to establish incentivized models for community-based sustainable mangrove forest and fisheries management. The national-level mangrove dynamics data detailed herein and complementary socioeconomic information highlighted three priority AOIs along the west coast of Madagascar for Blue Ventures' Blue Forest programme: Ambaro-Ambanja Bays (AAB), Mahajamba Bay (MHJ) and the Baie des Assassins (BdA) (Figure 1). The Tsiribihina and Manambolo Deltas (TMD) form a fourth AOI, where the localized mapping detailed herein is supporting WWF Madagascar West Indian Ocean Programme Office's work in the region. Each AOI encompasses the marine and terrestrial extent below 30 meters (m) elevation within 7 km of the coast.

AAB (centered at latitude 13°26'S, longitude 48°30'E) is comprised of two bays lined with extensive mangroves, which in aggregate form a contiguous ecosystem. AAB is most influenced by the Sambirano, Mananjeba, Mahavavy and Ifasy Rivers, with their headwaters in the Tsarantanana Massif mountain range to the southeast, including Maromokotro, Madagascar's highest peak at 2876 m. Situated at the convergence of the Sofia and Mahajamba rivers (centered at latitude 15°24'S, longitude 47°05'E), the tidal plains of MHJ encompass an extensive mangrove ecosystem. MHJ experiences a semidiurnal tidal range of 1.5–3 m (4–4.5 m during spring tide), an average surface water salinity range of 25–45 parts per thousand, and a mean annual precipitation of 1500 mm [73,74]. TMD (centered at latitude 19°36'S, longitude 44°27'E) is comprised of two deltas lined with extensive mangroves, forming a contiguous ecosystem. TMD is fed by the Mahajilo, Sakay, Kitsamby, Mania and Sakeny Rivers [87], with their headwaters in the Central Highlands (Ankaratra Massif [88]). The BdA (centered at latitude 22°12'S, longitude 43°17'E) is comprised of a single bay with a comparatively modest amount of mangroves, representing a contiguous ecosystem. A north-south rainfall gradient along the west coast results in a comparative abundance of precipitation in the north (e.g., AAB, MHJ and TMD), which contributes to higher stature mangrove trees than further south (e.g., BdA) [68,89].

2.2. Inventory and Comparison of Existing Data-Sets

Several studies have resulted in single- or multi-date national-level mangrove distribution maps for Madagascar (*i.e.*, [68,70–72]). Mayaux *et al.* [70] delineated mangrove and five other vegetation cover

types, circa 1998/1999, using 1 km Satellite Pour l'Observation de la Terre (SPOT) VEGETATION data. The Critical Ecosystem Partnership Fund (CEPF) [71] Madagascar Mapping Project mapped mangroves and 14 other vegetation types, circa 2001, with Moderate-resolution Imaging Spectroradiometer (MODIS) and Landsat data. Harper *et al.* [72] employed Landsat data to map forest cover, including mangroves, for 1973, 1990 and 2000. Giri and Muhlhausen [68] and Giri [69] utilized Landsat data to map mangrove and non-mangrove for 1973, 1990, 2000, 2005 and 2010. National-level dynamics calculated from these maps through 2005 are presented in Giri and Muhlhausen [68]). To date, no studies have reported on the nation-wide dynamics of Madagascar's mangroves beyond 2005.

Of the four specific AOIs, prior to 2014, AOI-specific maps existed for only MHJ and the BdA. For MHJ, Rasolofoharinoro *et al.* [73] employed Satellite Pour l'Observation de la Terre (SPOT) data to map seven intertidal vegetation zones for 1986 and 1993, which included four mangrove classes (*i.e.*, pioneering; dense mature; decaying; back (e.g., mangrove/terrestrial interface)). Pasqualini *et al.* [74] combined SPOT and radar data to delineate 10 coastal ecosystem types, circa 1993, including four morphologically (*i.e.*, frontal; interfluvial) and dynamics (*i.e.*, mature; recessive) related mangrove classes. Guillet *et al.* [75] utilized Landsat and SPOT data to map 12 coastal ecosystem classes, circa 1973, 1989, 2000 and 2006, including four mangrove types (*i.e.*, sparse *Avicennia marina*; average density *Avicennia marina*; dense *Avicennia marina*; and dense *Rhizophora mucronata*). For BdA, Roy *et al.* [90] used Quickbird (DigitalGlobe, Longmont, CO, USA) data to produce a map of mangrove and surrounding marine classes, circa 2005. These maps (*i.e.*, [73–75,90]) are no longer contemporary and/or unable to provide the thematic detail required for specific applications (e.g., carbon stock estimation).

As described in later sections, to improve upon the shortcomings associated with available maps for MHJ, Jones *et al.* [61] used Landsat data acquired in 2011 to produce a detailed, contemporary AOI-specific map of MHJ. Using similar methodologies, Jones *et al.* [25] produced an AOI-specific map for AAB from Landsat data acquired in 2010. At the time of writing, detailed contemporary maps existed for no other specific mangrove ecosystems in Madagascar; highlighting the need to produce new maps for TMD and BdA to complement those produced for AAB and MHJ.

2.3. National-Level Mangrove Distribution and Dynamics; Ecosystem-Level Dynamics

National-level data-sets were compared to determine which offered the most comprehensive (*i.e.*, in terms of their coverage of actual known mangrove area) and contemporary (*i.e.*, most recent) mangrove distributional information. Contemporary Landsat data, finer spatial resolution imagery viewable in Google Earth (Google, Mountain View, CA, USA) and extensive field observations were used to guide qualitative comparisons (Figure 2). Building on Giri and Muhlhausen [68], who reported mangrove extent circa 2005 and dynamics from 1990 to 2005, the maps deemed most comprehensive and contemporary were employed to establish contemporary (*i.e.*, beyond 2005) mangrove extent and quantify national-level mangrove dynamics (*i.e.*, loss, persistence and gain) from 1990 to 2010 using the Idrisi Land Change Modeler; a land planning and decision support tool (Clark Labs, Worcester, MA, USA). To investigate mangrove extent and dynamics at a finer scale, national-level mangrove data-sets were partitioned in to primary mangrove ecosystems, defined herein as individual ecosystems occupying at least 1000 ha and containing true mangroves: salt-tolerant halophytic trees and/or shrubs occurring entirely in tidal and inter-tidal areas [91].

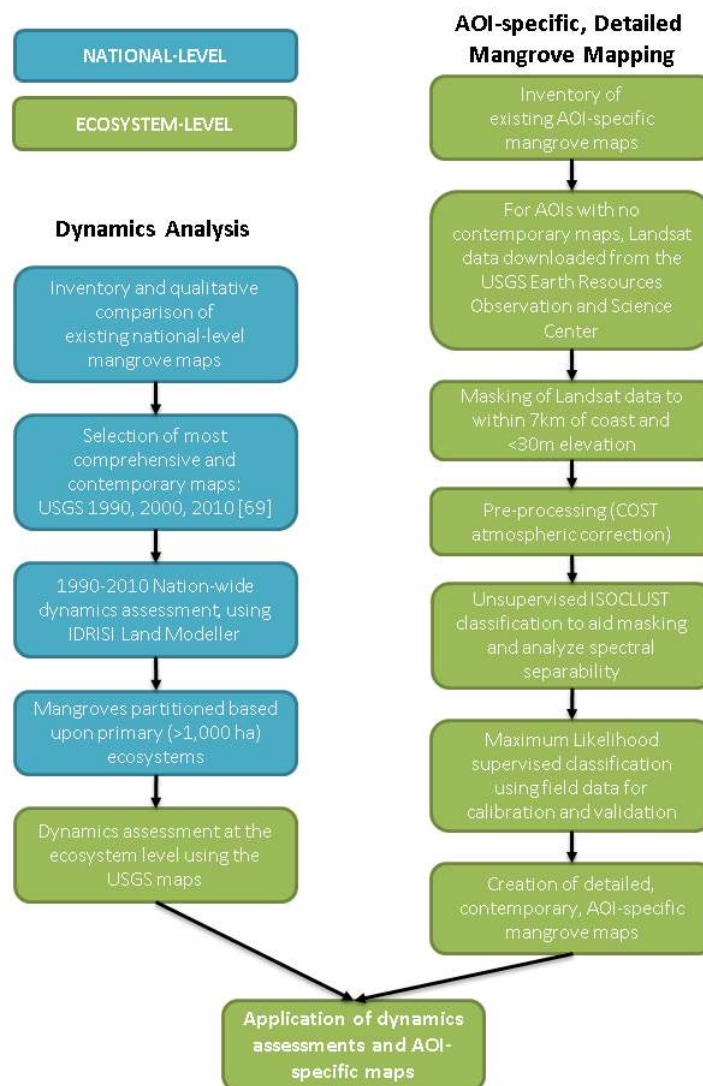


Figure 2. Workflow. Blue boxes represent national-level processing including the entire distribution of Madagascar’s mangroves. Green boxes represent ecosystem-level processing, including 30 primary mangrove ecosystems, with focus on four AOIs (*i.e.*, Ambaro-Ambanja Bays (AAB), Mahajamba May (MHJ), Tsiribihina-Manambolo Delta (TMD) and Baie des Assassins (BdA)). The results of nation-wide and ecosystem-specific dynamics from 1990 to 2010, and ecosystem-specific maps for TMD and BdA are presented in this study for the first time. The production of ecosystem-specific maps builds on previous studies which employed similar methods for AAB and MHJ (*i.e.*, Jones *et al.* [25]; Jones *et al.* [61]).

2.4. AOI-Specific Ecosystem-Level Mapping

2.4.1. Acquisition and Pre-Processing of Remotely Sensed Data

Following the methodology described in Jones *et al.* [25] for AAB, and Jones *et al.* [61] for MHJ, for mapping efforts in TMD and BdA, 30 m spatial resolution Landsat scenes were downloaded from the United States Geological Survey (USGS) Earth Resources Observation and Science Center (Sioux Falls, SD, USA) (Table 1). All Landsat scenes were orthorectified to a Shuttle Radar Topography Mission (SRTM) digital elevation model (DEM). Atmospheric correction was undertaken using the Cos(t) model [92], which estimates the impact of absorption by atmospheric gases and Rayleigh scattering, minimizes systematic haze, and converts image units to at-surface reflectance.

The bounding extent for all AOIs were established using distance to coastline (*i.e.*, 7 km) as an assumed mangrove habitat requirement [55,58,93]. Reducing the image extent based on habitat requirement through masking can increase classification accuracy by decreasing spectral confusion amongst target classes [57]. Emulating studies that establish the effectiveness of SRTM data to estimate mangrove forest canopy height (e.g., [94–98]), an SRTM height mask further eliminated unnecessary scene components based on a 30 m threshold, above which mangrove habitat were observed in each AOI not to exist [25,61].

Table 1. Summary of single-date Landsat scenes used for detailed, contemporary mapping of the four AOIs. Maps produced for Ambaro-Ambanja Bays (AAB) and Mahajamba Bay (MHJ) are originally described in Jones *et al.* [25] and Jones *et al.* [61]; whereas maps produced for Tsiribihina-Manambolo Delta (TMD) and Baie des Assassins (BdA) result from this study. Tide (m) indicates the average tidal height above mean sea level in or near the AOI during image acquisition.

AOI	Sensor	Date	Path/row	Tide (m)
AAB	Landsat 7 (L7) ETM	09/06/2010	159/69	1.9
MHJ	Landsat 5 (L5) TM	29/07/2011	160/71	1.7
TMD	Landsat 8 (L8) OLI	28/07/2014	161/73; 161/74	1.5
BdA	Landsat 8 (L8) OLI	23/04/2014	161/75	2.3

2.4.2. Initial Mapping; Definition and Refinement of Mangrove and Surrounding Land-Cover Categories

Adhering to the methods described in Jones *et al.* [25] for AAB, and Jones *et al.* [61] for MHJ, to produce initial maps for TMD and BdA, an unsupervised iterative self-organizing classification algorithm (*i.e.*, ISOCCLUS) was employed to group pixels in to dominant cover types based on shared spectral properties in bands 1–5 and 7 (*i.e.*, TM and ETM) or bands 2–7 (*i.e.*, OLI). Unsupervised classification for mapping mangroves and closely related ecosystem types is proven, and has produced both preliminary and final maps described in numerous studies [25,57,59,61,68,96,97,99–102]. Unsupervised classification results further facilitated masking based on areas dominated by water, cloud and/or shadow. Making reference to existing maps and finer spatial resolution imagery viewable in Google Earth, aggregation and iterative labelling was used to define and refine mangrove and surrounding land-cover types. Mangrove types varied slightly between AOIs, but were based on spectral differences attributable to ecological properties such as canopy-cover, stature and density (Table 2). All mangrove classes represent true mangroves and are assumed to be dominated by salt-tolerant halophytic trees and/or shrubs occurring entirely in tidal and inter-tidal areas [91]. Mangrove classes dominated by trees are considered forested stands; whereas classes dominated by shrubs/stunted trees do not meet international or national definitions for forest. Herein, the term mangrove ecosystem refers to a contiguous ecological unit containing both forest and non-forest areas of mangrove. Forested classes within a particular mangrove ecosystem are collectively referred to as mangrove forest.

In accordance with the approach described in Jones *et al.* [25] for AAB, and Jones *et al.* [61] for MHJ, to ensure the representativeness of and refine mangrove type and surrounding land-cover categories for TMD and BdA maps, preliminary field surveys were conducted in all four AOIs. Stratified random sampling was employed to target ha-sized reference plot locations within strata defined by the unsupervised classification results. Within mangrove reference plots established within each strata (Table 2), the height, diameter, canopy-cover, and crown dimensions were recorded for representative examples of each mangrove species present. Within non-mangrove reference plots, field notes and photographs recorded variability and confirmed representativeness. Within all reference plots, plot center was established with a Garmin GPSmap 62sc GPS unit left recording during the duration of measurements.

Table 2. Mapped classes, descriptions and 3 × 3 pixel calibration and validation reference areas for each of the four AOIs. Mapped classes for TMD and BdA build on previously published studies for AAB ([25]) and MHJ ([61]).

Area	Class	Description	Calibration	Validation	Total
AAB	Savannah	Dry grass, exposed soil, extremely sparse trees/shrubs	10	6	16
	Woodland	Dry grass and scattered trees/shrubs; canopy <30% closed	8	6	14
	Active cultivation	Dominated by pre-harvest agriculture (e.g., rice; sugar cane)	10	6	16
	Closed-canopy terrestrial forest	Stands of trees with well-formed canopies >60% closed	12	6	18
	Open-canopy terrestrial forest	Stands of trees/shrubs with canopies 30%–60% closed	8	6	14
	Closed-canopy mangrove	Tall, mature stands; canopy >60% closed	20	10	30
	Open-canopy mangrove I	Short-medium stands of trees/shrubs; canopy 30%–60% closed; moderately influenced by background soil/mud	15	9	24
	Open-canopy mangrove II	Stunted/short stands, shrub-dominant, very sparse; canopy ≥10% closed	11	6	17
	Deforested mangrove	Mosaic of stumps, scattered trees; canopy <30% closed	8	6	14
	Exposed soil	Inactive agri/aquacultural fields; extremely patchy savannah; extremely dry mud-flats	10	5	15
	Exposed mud	Mangrove/ocean interface; river sediment; wet mud-flats	8	5	13
		Total	120	71	191
MHJ	Active cultivation	Dominated by pre-harvest agriculture (e.g., rice)	14	7	21
	Closed-canopy terrestrial forest	Stands of trees with well-formed canopies >60% closed	14	7	21
	Open-canopy terrestrial forest	Stands of trees/shrubs with canopies 30%–60% closed	16	8	24
	Closed-canopy mangrove I	Tall, mature stands; canopy >80% closed	22	10	32
	Closed-canopy mangrove II	Tall, mature stands; canopy >60% closed	22	10	32
	Open-canopy mangrove I	Short-medium stands of trees/shrubs; canopy 30%–70% closed; moderately influenced by background soil/mud	14	7	21
	Open-canopy mangrove II	Short-medium stands of trees/shrubs; canopy 30%–70% closed; significantly influenced by background soil/mud	12	7	19
	Open-canopy mangrove III	Stunted/short stands, shrub-dominant, very sparse; canopy <30% closed	14	7	21
	Exposed soil	Inactive agri/aquacultural fields; sparsely vegetated, soil-dominated areas; dry mud-flats	21	10	31
	Exposed mud	Mangrove/ocean interface; river sediment; wet mud-flats; inactive aquaculture ponds	14	7	21
		Total	163	80	243

Table 2. Cont.

Area	Class	Description	Calibration	Validation	Total
TMD	Dense mangrove	Tall, mature stands; canopy >70% closed	16	6	22
	Sparse mangrove	Short-medium stands of trees/shrubs; canopy 30%–70% closed; moderately influenced by background soil/mud	12	5	17
	Bare type I	Exposed soil; scrub mangrove; mud-flats; fallow agriculture; patchy grass/bushland	14	6	20
	Dense terrestrial forest	High-stature terrestrial trees with well-formed canopies	12	6	18
	Sparse terrestrial forest	Mixed-stature terrestrial trees with relatively open canopies interspersed with wooded grassland-bushland	10	5	15
	Wooded grassland-bushland	Grassland and/or bush-land	10	5	15
	Active agriculture	Dominated by pre-harvest agriculture (e.g., rice)	3	1	4
	Bare type II	Typically dry soil and/or sand; extremely dry patchy grass/bushland	10	5	15
		Total	87	39	126
BdA	Spiny forest	Moderate-high stature, relatively closed-canopy stands	9	3	12
	Barren/exposed	Dominance of rock, sand, dry soil; interspersed with sparse vegetation	9	3	12
	Cultivated/degraded/woodland	Active or fallow cultivation; degraded and/or sparse terrestrial forest; woodland	9	3	12
	Burnt	Areas which have recently experienced fire	9	3	12
	Water dominated	Water dominant; mud-flats	10	4	14
	Closed-canopy mangrove	Tall, mature stands; canopy >60% closed	9	3	12
	Open-canopy mangrove I	Short-medium stands of trees/shrubs; canopy 30%–70% closed; influenced by background soil/mud	9	3	12
	Open-canopy mangrove II	Stunted/short stands; shrub-dominant, very sparse; canopy <30% closed	9	3	12
		Total	73	25	98

2.4.3. Supervised Image Classification

As with previously reported mapping efforts in AAB and MHJ, for TMD and BdA, reference plots facilitated both calibrating the spectral properties of different mangrove and surrounding land-cover types for image classification (*i.e.*, calibration) and assessing resulting map accuracy (*i.e.*, validation). By exploiting the familiarity gained with the appearance and location of target classes, supplemental reference areas were located in finer spatial resolution imagery viewable in Google Earth for all mapped categories. Reference areas were spread throughout and randomly partitioned to facilitate both calibration and validation (Table 2). In adherence with methods described in Jones *et al.* [25] for AAB, and Jones *et al.* [61] for MHJ, for TMD and BdA, supervised classification of Landsat data was employed to produce maps of class distributions using the maximum likelihood (ML) algorithm. Numerous studies have shown the effectiveness of ML for classifying mangrove habitat with Landsat-like data [25,58,60,61,73,95,103–108]. The accuracies of resulting maps were quantified using confusion matrices, which cross-tabulate independent validation data against mapped classes. The Kappa index of agreement further assessed how much better than random each map was [109].

3. Results and Discussion

3.1. Overview of Existing National-Level Maps and Data-Sets

A qualitative comparison of existing national-level mangrove data-sets (*i.e.*, [68,70–72]) concluded that those produced by the USGS (*i.e.*, [69]) offered the most comprehensive historic and contemporary areal estimates of Madagascar’s mangroves (Figure 3). Crucially, the USGS produced maps were the only ones to provide relatively contemporary (*i.e.*, 2010) distribution and focus solely on mangroves, with all other national-level maps representing multiple forest types and time periods nearly or greater than 10 years earlier. Thus, the USGS data-sets were utilized for all consequent dynamics analyses. Additional details regarding comparisons between Madagascar’s existing national-level mangrove data-sets are available in Giri and Muhlhausen [68], Jones *et al.* [25] and Jones *et al.* [61]. Further details outlining loss calculated for Madagascar’s mangroves using USGS maps through to 2005 is available in Giri and Muhlhausen [68].

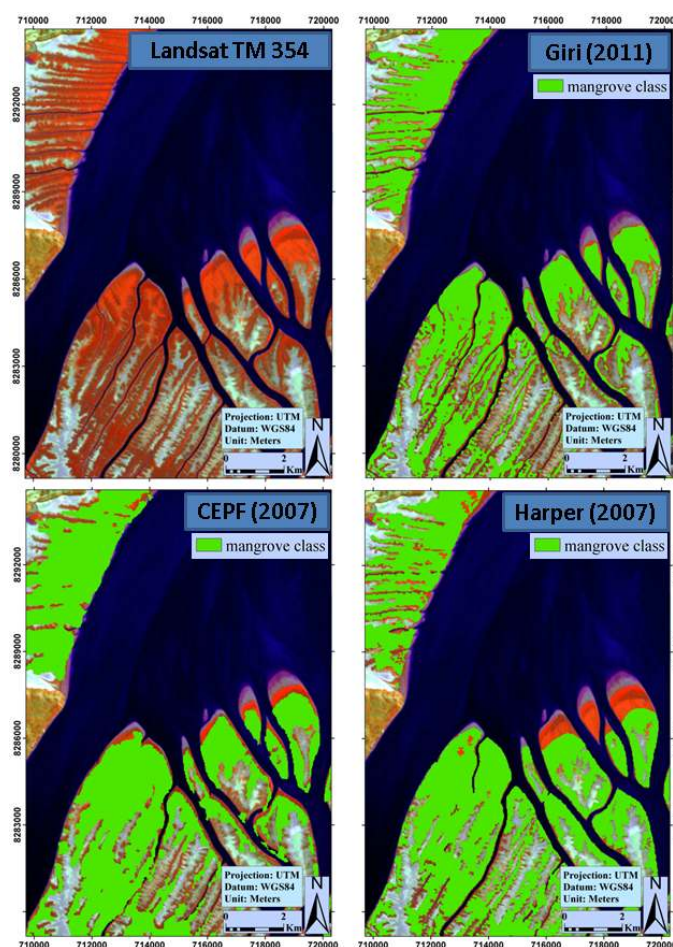


Figure 3. A Landsat TM Blue-Green-Red 354 false color composite from July, 2011 is shown in the top left panel wherein mangroves appear primarily in shades of red. Mangrove coverage from three national data-sets (*i.e.*, Giri [69]; CEPF [71]; Harper *et al.* [72]) is overlain on the Landsat composite in the three other panels. This comparison illustrates how data produced by Giri [69] provide the most comprehensive (in terms of representing actual known mangrove area) and contemporary (in terms of year) mangrove coverage; as is illustrated by the variably represented mangrove covered islands in the middle-right of each panel. The area shown in all four panes is a portion of MHJ.

3.2. Mangrove Distribution and Dynamics: 1990–2010

3.2.1. National-Level Distribution and Dynamics

According to the USGS-produced Landsat-derived maps of national-level mangrove coverage from 1990, 2000 and 2010 [69], as of 2010 Madagascar contained approximately 213,000 ha of mangrove ecosystems distributed primarily along the west coast, with scattered, isolated pockets found on the north east coast (Figure 1). Analysis of the 1990, 2000 and 2010 USGS maps indicates that from 1990 to 2010, there was a country-wide net loss (*i.e.*, loss-gain) of 21% (*i.e.*, 57,359 ha).

3.2.2. Ecosystem-Level Dynamics

Considered independently, there are nearly 100 distinct, non-contiguous mangrove ecosystems in Madagascar; however, over 200,000 ha (*circa* 2010) are represented by 30 primary ecosystems, each greater than 1000 ha in size. Of these primary ecosystems, according to the USGS maps, as of 2010, MHJ had the greatest extent (*i.e.*, 26,667 ha), followed by AAB (*i.e.*, 25,664) and TMD (*i.e.*, 20,242 ha) (Table 3; Figure 4). BdA, ranked as Madagascar's 26th largest mangrove ecosystem, containing 1362 ha as of 2010. The extent in ha for 1990, 2000 and 2010 according to USGS-produced maps as partitioned by primary mangrove ecosystems are provided in Table 3 and Figure 4.

As previously reported in Jones *et al.* [25], and Jones *et al.* [61], in AAB, the analysis of USGS maps suggest a loss of 7659 ha (23.7%) and gain of 995 ha (3.1%) from 1990 to 2010 (Figure 5). Deforestation is mostly occurring on or near the peninsular base, which separates the two Bays. As described in Jones *et al.* [61], for MHJ, analyzing the USGS maps indicate 1251 ha were lost (4.5%) and 150 gained (0.5%) from 1990 to 2010 (Figure 5). As compared with other primary mangrove ecosystems in Madagascar, notably AAB, MHJ's mangroves have remained comparatively stable. Comparisons with terrestrial data (*i.e.*, [72]) also imply that from 2000 to 2005 alone, loss in the terrestrial forests surrounding MHJ exceeded mangrove loss from 2000 to 2010. However, mangrove loss in MHJ does appear to be increasing, particularly in the east. For TMD, the analysis of the USGS maps indicated a net loss of 12,612 ha (38.4%) from 1990 to 2010 (Figure 5). For BdA, analyzing the USGS maps indicated that from 1990 to 2010 there was a net loss of 360 ha (20.9%) (Figure 5).

Table 3. The extent in hectares for Madagascar's primary mangrove ecosystems for 1990, 2000 and 2010, based on partitioning USGS-produced Landsat-derived national-level mangrove cover maps for 1990, 2000 and 2010 [69] in to primary (*i.e.*, >1000 ha) mangrove ecosystems. Extents are ordered from largest to smallest based on 2010 values.

Mangrove ecosystem	Mangrove Extent (Hectares)		
	1990	2000	2010
<i>Mahajamba Bay (MHJ)</i>	27778	27577	26677
<i>Ambaro-Ambanja Bays (AAB)</i>	32328	30321	25664
<i>Tsiribihina and Manambolo Deltas (TMD)</i>	32854	24651	20242
Antsohihy	17081	16065	13838
Tambohorano	21140	12781	13418
Sahamalaza	12107	11063	10956
Mahavavy su Sud	10615	10870	10654
Mahajanga	12375	11814	9574
Mangoky	14684	12247	9431
Morondava-Bosy	8743	7500	6123
Kamendriky-Tsilambana	6102	6102	5924
Mahabo-Andramy	4721	5939	5905
Maintirano	8937	4644	5900
Boeny	3870	3888	3867

Table 3. Cont.

	Mangrove Extent (Hectares)		
Baly-Soalala	3687	3683	3507
Besalampy	6247	5097	3287
Rigny-Irody	3224	3232	3231
Morombe	3652	2952	3035
Mariarano	2472	2412	2330
Narinda	2249	2058	2036
Sohany	2470	1984	2025
Belo sur Mer	2603	2387	1917
Vilamatsa	1881	1881	1847
Kabatomena	2458	1882	1529
Reharaka	2229	1528	1406
<i>Baie des Assassins (BdA)</i>	1723	1301	1362
Manampatra	1405	1404	1327
Morovasa	1253	1199	1199
Mangolovo	1415	981	1172
Ambondrombe	1462	1349	1109
Total	253,765	220,792	200,492

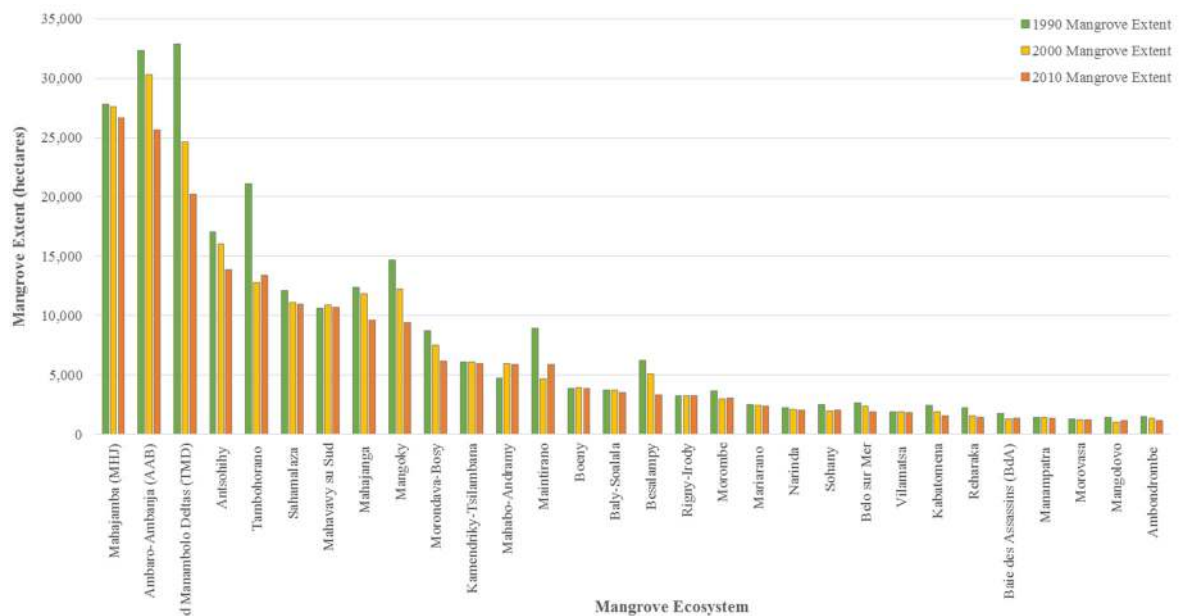


Figure 4. The extent in hectares for Madagascar's primary mangrove ecosystems for 1990, 2000 and 2010, based on partitioning USGS-produced Landsat-derived national-level mangrove cover maps for 1990, 2000 and 2010 [69] in to primary (*i.e.*, >1000 ha) mangrove ecosystems. Extents are ordered from largest to smallest based on 2010 values.

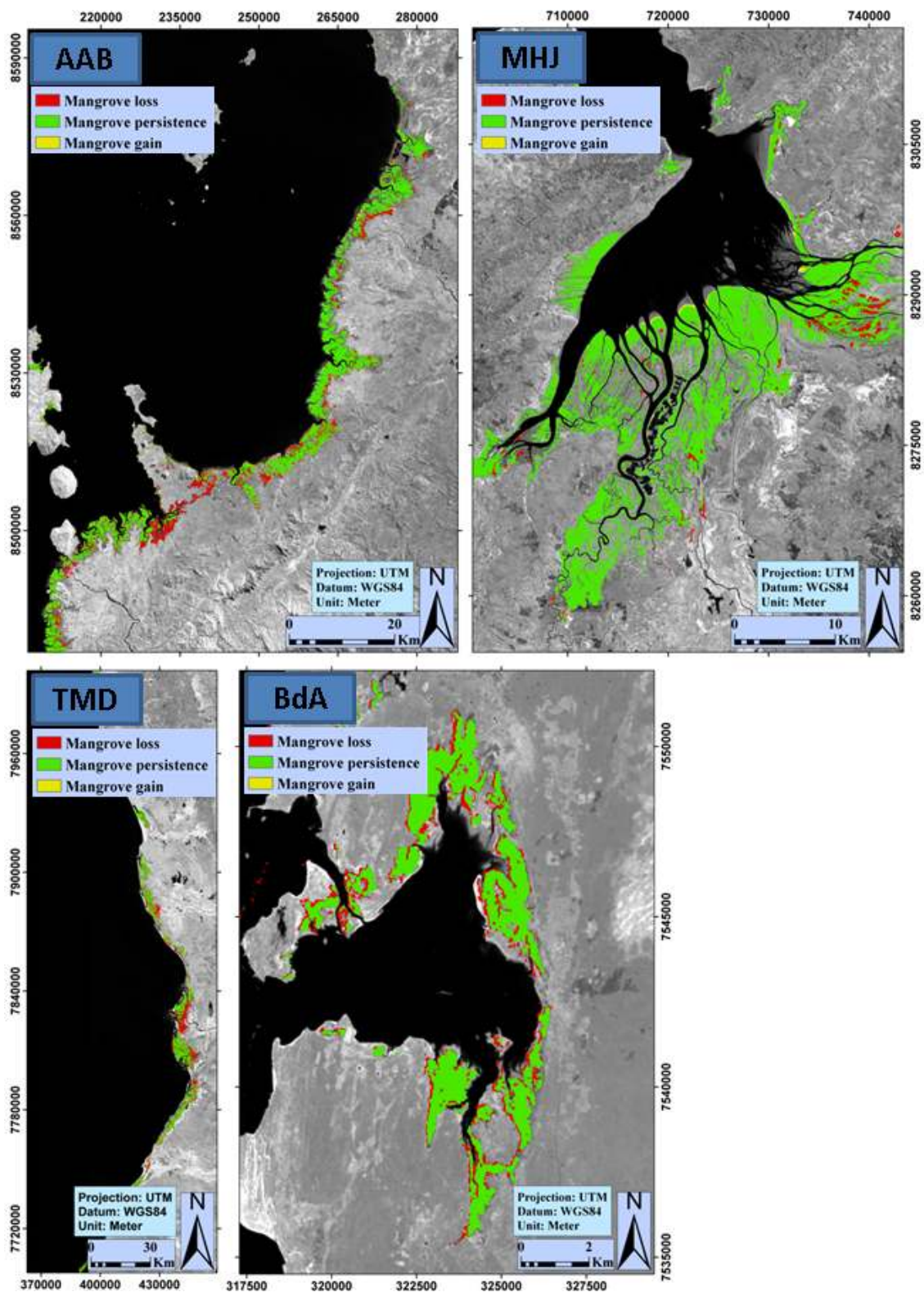


Figure 5. Dynamics from 1990 to 2010 for each of four AOIs calculated using the USGS-produced, Landsat-derived mangrove cover maps for 1990, 2000 and 2010 [69]. Background images are Landsat NIR bands from AOI-specific dates provided in Table 1.

3.3. AOI-Specific Ecosystem-Level Mapping Results

3.3.1. Spectral Separability and Classification Results

As demonstrated through results initially presented in Jones *et al.* [25] for AAB, and Jones *et al.* [61] for MHJ (Figure 6), for TMD and BdA, all mapped classes are spectrally separable using specific portions of the electromagnetic spectrum as represented by certain Landsat bands. In particular, the near-infrared (NIR) and short-wave infrared (SWIR) were useful for distinguishing between mangrove types and differentiating mangroves from surrounding mapped categories. In the NIR (0.76–0.90 micrometers (μm)), the spectral distinctiveness of mangrove classes was probably driven by vegetative reflectance relating to the transitional red-edge, internal vegetation structure, and leaf dry-matter content [15,69,99,110]. In the SWIR (1.55–1.75 and 2.08–2.35 μm), differences in reflectance were driven by vegetation and soil moisture content, and canopy-level biogeochemical constituents likely facilitated mangrove differentiation [100]. These results further support previous studies, which demonstrate that SWIR wavelengths help distinguish mangroves from surrounding terrestrial vegetation [25,111]. Mangroves types were also further differentiated in the visible bands (*i.e.*, blue: 0.45–0.52 μm , green: 0.53–0.61 μm , and red: 0.63–0.69 μm).

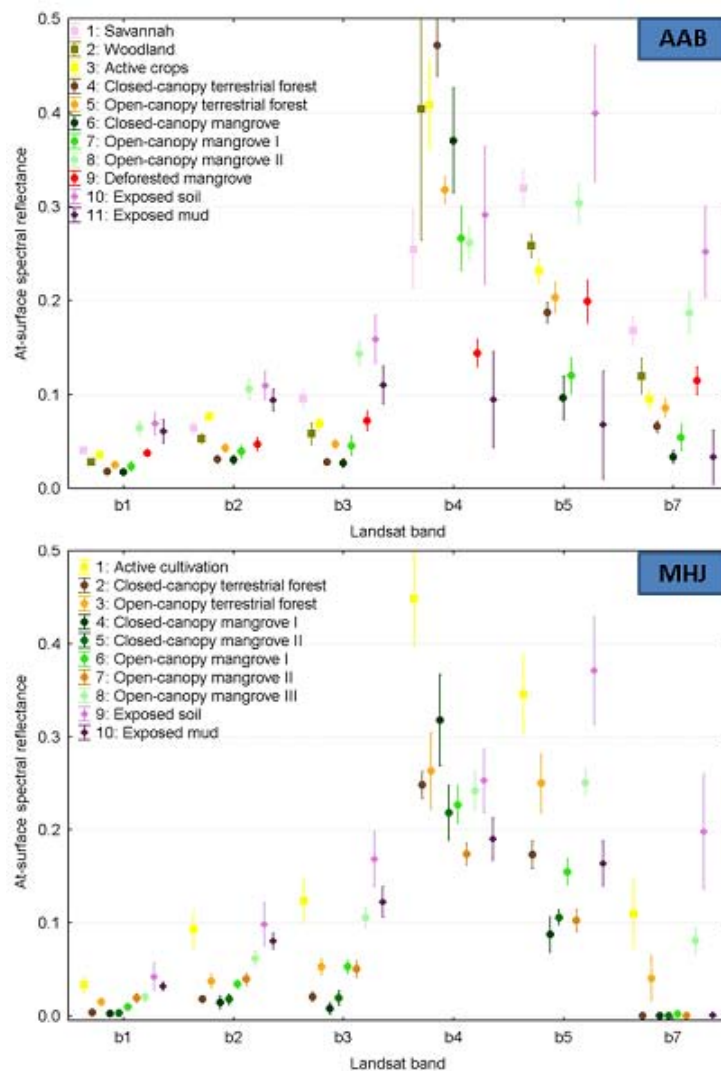


Figure 6. The mean spectral reflectance (± 1 standard deviation) of mapped classes for Ambaro-Ambanja Bays (AAB) and Mahajamba Bay (MHJ) (adapted from [25,61]).

In support of results originally described in Jones *et al.* [25] for AAB, and Jones *et al.* [61] for MHJ, ML classification for TMD and BdA resulted in highly accurate AOI-specific maps (Table 4; Figure 7). Our results further indicate that while common as a source of classification error in mangrove studies, confusion with other vegetation classes (e.g., terrestrial forest types) was mostly avoided. As compared with single-class contemporary (*i.e.*, 2010) mangrove coverage provided by the USGS national-level map, it is clear that our classification results provide more detailed and comprehensive representation of mangroves (Figure 8). In total, USGS maps imply 25,664, 26,677, 20,242 and 1362 ha of mangroves for AAB, MHJ, TMD and BdA, respectively. In contrast, AOI-specific maps imply 45,680, 45,107, 28,513, and 1652 ha of mangrove ecosystem for AAB, MHJ, TMD and BdA, respectively. When considering mangrove forest only and excluding classes dominated by shrub/scrub, the amount of mangroves in each AOI is reduced but still markedly higher than USGS estimates (Figure 9). The USGS map under-represents mangrove stands which are naturally lower stature and more open or highly degraded, and completely omits most scrub/shrub-dominated areas and certain narrow linear strips. The under-representation results in conservative distribution estimates, which in turn impacts ranking primary mangrove ecosystems by extent, as undertaken in this study. This is exemplified by MHJ being estimated as Madagascar's largest mangrove ecosystem based on the USGS map; whereas our AOI-specific map indicates that AAB was slightly larger.

Under-representation of lower stature or sparser mangrove areas associated with national-level USGS maps can also exaggerate dynamics by indicating loss in areas that may actually represent degradation or sparse areas of mangrove on the edge of the limits of detection by the automated algorithms used to create the data. Field observations confirm that certain areas appearing as loss in the USGS maps were in actuality occupied by sparse or degraded mangroves. In addition, given that numerous Landsat images were mosaicked together for each temporal increment to create the USGS maps, the influence of different dates and thus tidal conditions may have also exaggerated dynamics. The potential for exaggerated dynamics in the USGS maps needs to be taken in to account when considering the national-level dynamics presented in this study; though concerns of exaggerated loss must be tempered with an acknowledgement of an under-representation of sparse and degraded mangroves, which leads to initial under-estimates of mangrove distributions from which dynamics are calculated. Bearing in mind the limitations of the single mangrove class represented by the USGS maps, they also provide no context regarding surrounding land-cover categories, including extensive mud flats that once were or could again become mangrove ecosystems. In aggregate, these shortcomings highlight the importance of detailed, contemporary ecosystem-specific localized mapping; which is bolstered by USGS maps being >four years old, providing outdated representation for ecosystems which continue to experience increased and widespread degradation and deforestation.

Table 4. (a–d) Classification accuracies, including overall accuracies, Kappa statistics and per-class user’s and producer’s accuracies. Results for AAB and MHJ were previously reported in Jones *et al.* [25] and Jones *et al.* [61].

(a)															
Area:	Class:	1	2	3	4	5	6	7	8	9	10	11	Total	User’s (%)	Commission (%)
AAB:	Savannah (1)	54	3	0	0	0	0	0	0	0	1	0	58	93	7
	Woodland (2)	0	39	0	0	0	0	0	0	0	0	0	39	100	0
	Active cultivation (3)	0	0	51	0	0	0	0	0	0	0	0	51	100	0
	Closed-canopy terrestrial forest (4)	0	0	0	54	0	0	0	0	0	0	0	54	100	0
	Open-canopy terrestrial forest (5)	0	4	0	0	54	0	0	0	0	0	0	58	93	7
	Closed-canopy mangrove (6)	0	0	0	0	0	79	9	0	0	0	0	88	90	10
	Open-canopy mangrove I (7)	0	0	0	0	0	11	72	0	2	0	0	85	85	15
	Open-canopy mangrove II (8)	0	0	0	0	0	0	0	52	0	0	0	52	100	0
	Deforested mangrove (9)	0	0	0	0	0	0	0	0	60	0	0	60	100	0
	Exposed soil (10)	0	8	3	0	0	0	0	2	1	53	0	67	79	21
	Exposed mud (11)	0	0	0	0	0	0	0	0	0	0	54	54	100	0
Total		54	54	54	54	54	90	81	54	63	54	54	666		
Producer’s (%)		100	72	94	100	100	88	89	96	95	98	100	Overall Accuracy = 93.4%		
Omission (%)		0	28	6	0	0	12	11	4	5	2	0	Kappa = 0.9		

(b)															
Area:	Class:	1	2	3	4	5	6	7	8	9	10	Total	User’s (%)	Commission (%)	
MHJ:	Active cultivation (1)	63	0	0	0	0	0	0	0	0	0	63	100	0	
	Closed-canopy terrestrial forest (2)	0	62	0	0	0	0	0	0	0	0	62	100	0	
	Open-canopy terrestrial forest (3)	0	1	72	0	0	3	0	1	0	0	77	94	6	
	Closed-canopy mangrove I (4)	0	0	0	90	2	0	0	0	0	0	92	98	2	
	Closed-canopy mangrove II (5)	0	0	0	0	88	0	0	0	0	0	88	100	0	
	Open-canopy mangrove I (6)	0	0	0	0	0	60	0	0	0	0	60	100	0	
	Open-canopy mangrove II (7)	0	0	0	0	0	0	60	0	0	0	60	100	0	
	Open-canopy mangrove III (8)	0	0	0	0	0	0	0	62	0	0	62	100	0	
	Exposed soil (9)	0	0	0	0	0	0	0	0	90	0	90	100	0	
	Exposed mud (10)	0	0	0	0	0	0	3	0	0	63	66	95	5	
	Total		63	63	72	90	90	63	63	63	90	63	720		
Producer’s (%)		100	98	100	100	98	95	95	98	100	100	Overall Accuracy = 98.6%			
Omission (%)		0	2	0	0	2	5	5	2	0	0	Kappa = 0.9			

Table 4. Cont.

(c)												
Area:	Class:	1	2	3	4	5	6	7	8	Total	User's (%)	Commission (%)
	Dense mangrove (1)	54	0	0	0	0	0	0	0	54	100	0
	Sparse mangrove (2)	0	45	0	0	0	0	0	0	45	100	0
	Bare type I (3)	0	0	52	0	0	0	0	0	52	100	0
	Dense forest (4)	0	0	0	54	0	0	0	0	54	100	0
	Sparse forest (5)	0	0	0	0	45	0	0	0	45	100	0
TMD:	Wooded grassland-bushland (6)	0	0	0	0	0	45	0	0	45	100	0
	Active agriculture (7)	0	0	0	0	0	0	9	0	9	100	0
	Bare type II (8)	0	0	2	0	0	0	0	48	50	96	4
	Total	54	45	54	54	45	45	9	48	354		
	Producer's (%)	100	100	96	100	100	100	100	100		Overall Accuracy = 99.4%	
	Omission (%)	0	0	4	0	0	0	0	0		Kappa = 0.99	
(d)												
Area:	Class:	1	2	3	4	5	6	7	8	Total	User's (%)	Commission (%)
	Spiny forest (1)	27	0	0	0	0	0	0	0	27	100	0
	Barren/exposed (2)	0	30	0	0	0	0	0	0	30	100	0
	Cultivated/degraded/woodland (3)	0	0	27	0	0	0	0	0	27	100	0
	Burnt (4)	0	0	0	27	0	0	0	0	27	100	0
	Water dominated (5)	0	0	0	0	42	0	0	0	42	100	0
BdA:	Closed-canopy mangrove (6)	0	0	0	0	0	27	0	0	27	100	0
	Open-canopy mangrove I (7)	0	0	0	0	0	0	27	0	27	100	0
	Open-canopy mangrove II (8)	0	0	0	0	0	0	0	27	27	100	0
	Total	27	30	27	27	42	27	27	27	234		
	Producer's (%)	100	100	100	100	100	100	100	100		Overall Accuracy = 100	
	Omission (%)	0	0	0	0	0	0	0	0		Kappa = 1	

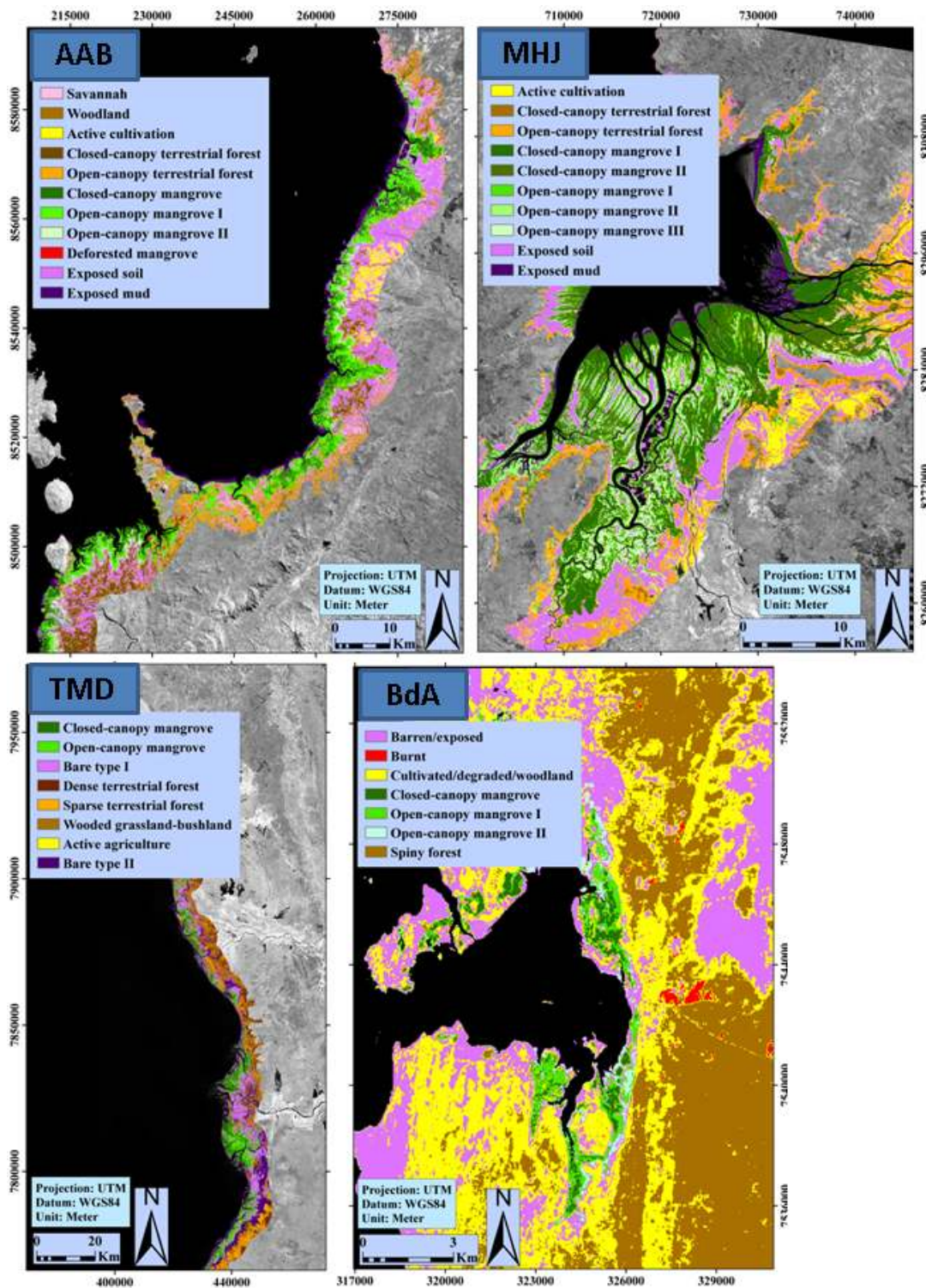


Figure 7. The results of detailed, contemporary, ecosystem-level mapping for four AOIs (*i.e.*, Ambaro-Ambanja Bays (AAB), Mahajamba bay (MHJ), Tsiribihina Manambolo Delta (TMD), and Baie des Assassins (BdA)). The water dominated class is excluded for BdA and is excluded from the figure. For each AOI, the background image is a Landsat NIR band (*i.e.*, band 4: Landsat 5 TM and Landsat 7 ETM+ ; band 5: Landsat 8 OLI) as described in Table 2. Mapping results for AAB and MHJ were originally presented in Jones *et al.* [25] and Jones *et al.* [61].

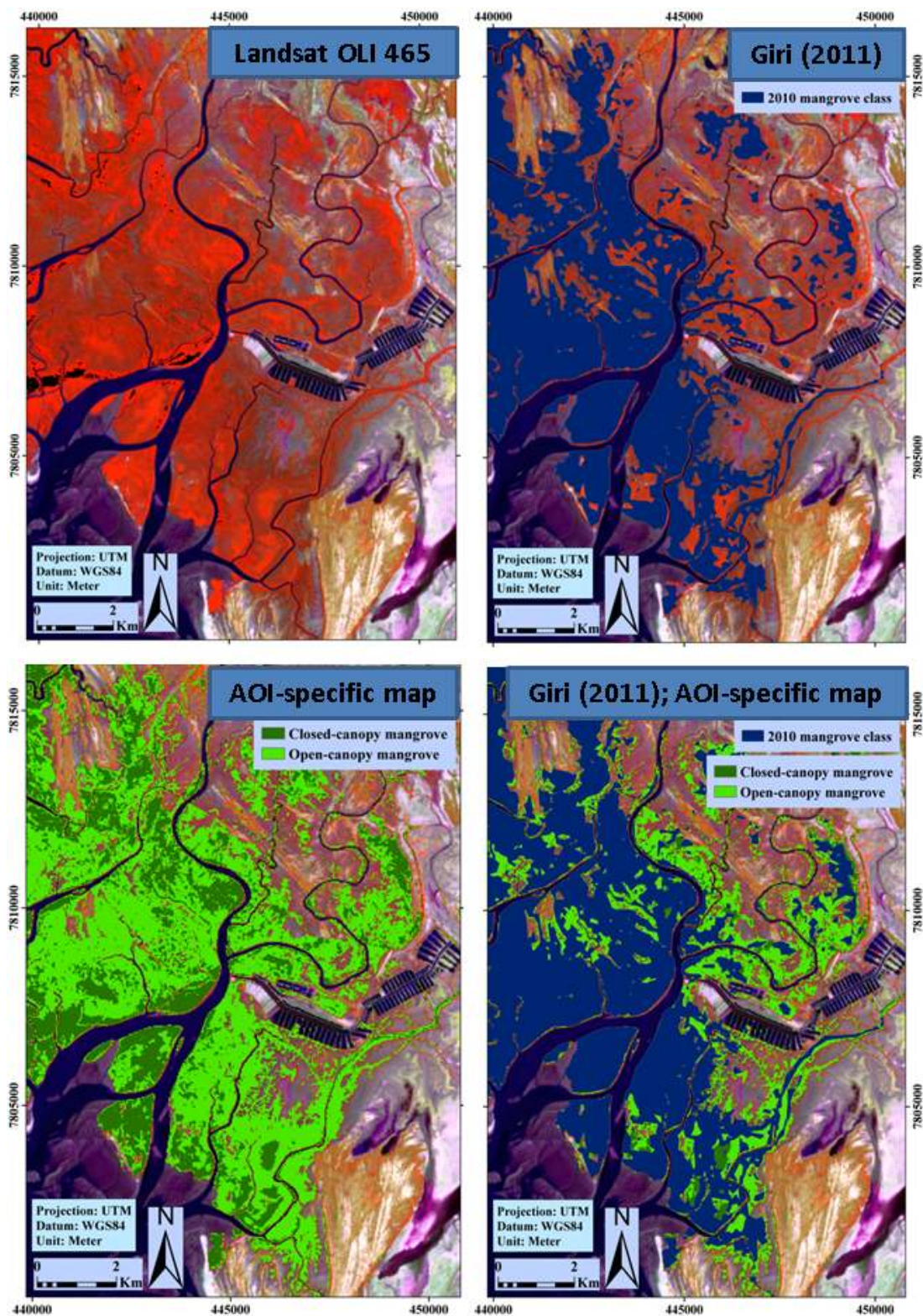


Figure 8. A Landsat OLI 465 false color composite from July, 2014, over the Tsiribihina-Manambolo Delta (TMD) AOI, is shown in the top left panel, wherein mangroves appear primarily in shades of red. The other panels compare USGS-produced national-level mangrove coverage *circa* 2010 (Giri [69]) to one of the detailed, contemporary, AOI-specific maps produced through this study. The comparison demonstrates how the USGS map (Giri [69]) underrepresents naturally lower stature, more open or highly degraded mangroves and at times omits scrub/shrub and narrow linear strips of mangroves.

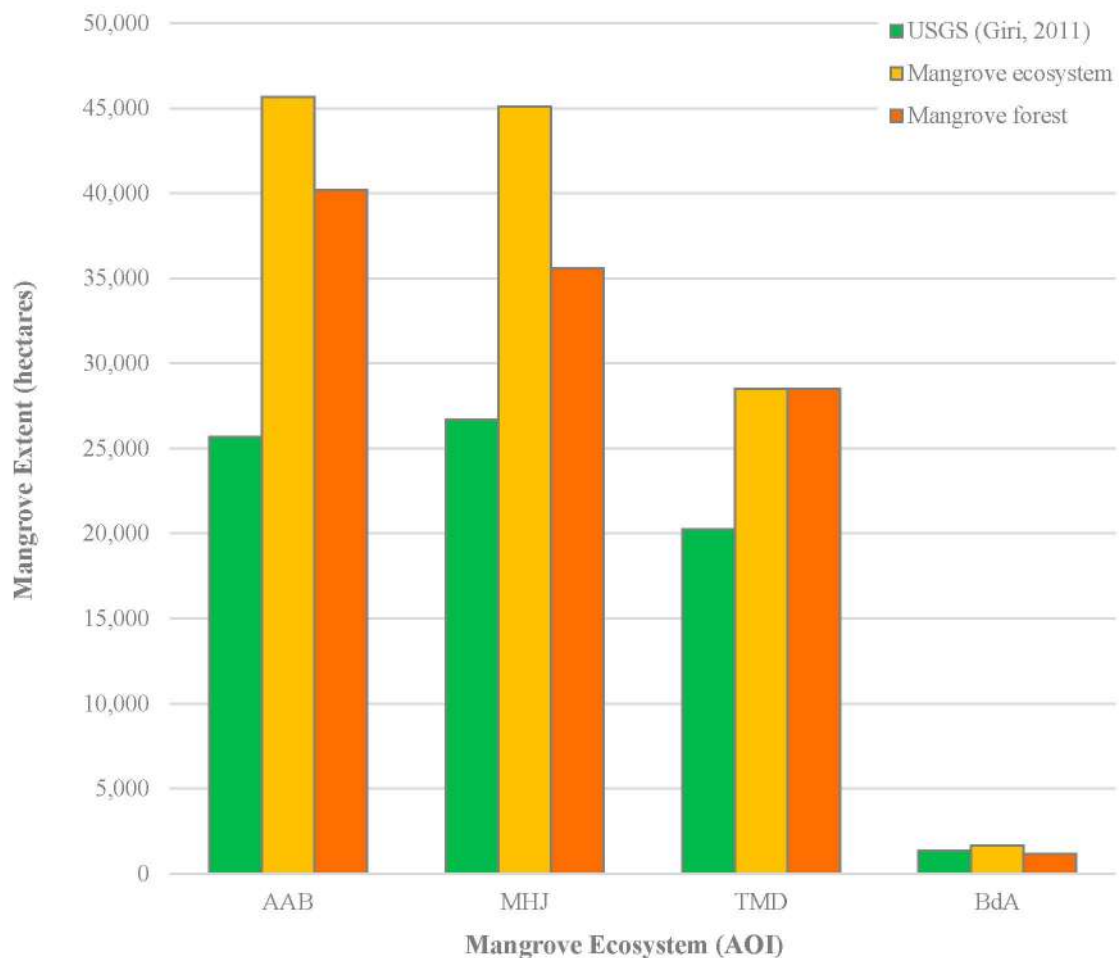


Figure 9. The extent of mangroves based on the 2010 national-level USGS-produced Landsat derived mangrove cover map [69] versus the results of AOI-specific contemporary mapping is shown for each AOI. For AOI-specific mapping results, extent is shown based on all mangrove classes including shrub/scrub dominated (*i.e.*, mangrove ecosystem) and based on only classes meeting the definition of forest (*i.e.*, mangrove forest).

3.3.2. Application of Mapping Results

The results of the national- and ecosystem-level dynamics analysis described in Section 3.2 have supported Blue Venture’s Blue Forests programme in selecting areas in critical need of mangrove conservation and restoration. The contemporary AOI-specific maps described in Section 3.3 are being applied for ecological characterization and carbon stock estimation, to provide baselines for historical mapping/future monitoring, and to support the establishment of carbon projects.

As described in Jones *et al.* [25] for AAB, and Jones *et al.* [61] for MHJ, localized mangrove maps were used to stratify mangroves and systematically establish carbon plots based on adaptations of methods proposed by the Centre for International Forestry Research (CIFOR) as outlined in Kauffman and Donato [24]. In total, 55 and 51 carbon plots were established for AAB and MHJ, respectively. Tree measurements summed at the plot-level allowed for summarizing the primary ecological characteristics of each mapped mangrove type, and allowed breaking mangrove classes into sub-types based on dominant ecological traits (Table 5). Open-canopy areas were typically comprised of sparse and mostly stunted/shrub, low stature mangroves with very open canopies or moderately-dense stands of medium stature trees with relatively open canopies. In contrast, closed-canopy areas were typified by higher stature trees of variable density with well-formed canopies.

Exceptions to these typical ecosystem characteristics included, (1) areas dominated by extremely dense, closed-canopy medium/near-tall trees and (2) mature stands which were either highly degraded or naturally open, both of which can spectrally appear as open-canopy mangrove. This overlap highlights a distinct limitation of our maps, which is the inability to reliably detect and distinguish mangrove degradation. While field observations confirm that degradation exists in all AOIs, of both natural and anthropogenic in origin, the full extent of degradation remains uncertain. While mangrove conversion (*i.e.*, deforestation) can be reliably mapped and monitored with moderate resolution data (e.g., Landsat) using established methods, accurately detecting and tracking the subtle sub-pixel modification (*i.e.*, degradation) of mangrove ecosystems remains a vexing challenge. Finer spatial resolution imagery can be employed to accurately detect tree-level degradation, but these data remain prohibitively expensive for small or not-for-profit organizations. Directly incorporating other remotely sensed data-sets, such as those representing forest structure (e.g., LiDAR; radar), into the classification process could greatly increase explanatory power and help further sub-divide existing classes based on degradation; though access to such complimentary data-sets remains limited. Even if able to accurately detect degradation, it would remain difficult to confidently partition natural *versus* anthropogenic. Despite the limitations of our mangrove classes, they are spectrally distinct and field observations confirm that they are ecologically different and meaningful.

For AAB and MHJ, the tree diameter and height measurements collected in plots were used as input in allometric equations to calculate above-ground biomass and estimate carbon stocks. Tree below-ground biomass was calculated with a generalized equation presented in Komiyama *et al.* [112]. Equations found in Kauffman and Donato [24] were used to estimate the biomass of standing dead wood. Soil samples taken at the center of each plot allow for the determination of soil organic carbon (SOC), which is still ongoing. For AAB, preliminary SOC was estimated using a modified Walkley-Black method [113–115] from samples sent to the Laboratoire des Radio Isotopies (LRI) in Antananarivo, Madagascar. Estimates of carbon calculated based on plot measurements in all AOIs were scaled to the ha-level.

As presented in Jones *et al.* [61,62], and representing the first total carbon stock estimates for a mangrove ecosystem in Madagascar, total carbon stock estimates in AAB varied from 126.42 to 570.72 Mg·C·ha⁻¹, with an overall mean of 356.36 (±16.96) Mg·C·ha⁻¹ (Figure 10). Average vegetation carbon was highest within the tall-stature closed-canopy mangroves (114.8 (±9.3) Mg·C·ha⁻¹). In comparison, open-canopy I and open-canopy II mangroves had average vegetation C values of 43.6 (±7.3) Mg·C·ha⁻¹ and 19.3 (±4.6) Mg·C·ha⁻¹ respectively. Mean SOC values, based on soil depth up to 100 cm, ranged from 165.2 (±29.1) Mg·C·ha⁻¹ for open-canopy II mangroves, to 278.80 (±20.99) Mg·C·ha⁻¹ for open-canopy I mangroves, and 309.87 (±19.36) Mg·C·ha⁻¹ for closed-canopy mangroves. Total carbon stock estimates of trees (*i.e.*, above- and below-ground) in MHJ varied from 2.97 to 279.49 Mg·C·ha⁻¹, with an overall mean of 100.96 (±10.49) Mg·C·ha⁻¹ (Jones *et al.* [61,62]) (Figure 11). The closed-canopy I class, wherein tree stature was largest and tree density highest, had the highest carbon values (166.82 (±15.38) Mg·C·ha⁻¹).

The differences in carbon stock estimates between closed- and open-canopy classes in AAB and MHJ (Figure 11) reflect variable forest stature and density and supports that larger, taller, denser trees contain significantly greater amounts of carbon. The difference in carbon stocks between the two AOIs is influenced by disproportionate amounts of higher stature trees in MHJ as compared with AAB. Collectively, these estimates support a growing body of evidence that mangroves are amongst the most carbon-dense forests in the tropics, with similar above- and larger below-ground stocks than terrestrial tropical upland systems [14,17,21–23,116–121].

Table 5. Mangrove class, species dominance, average tree height (m) (\pm standard error (SE)), average dbh (cm) (\pm SE) and average trees per hectare (ha^{-1}) (\pm SE) for mapped mangrove categories. Adapted from Jones *et al.* [25] and Jones *et al.* [61].

Class	Code	Description	Species Dominance	N	Average Tree Height (m)	Average dbh (cm)	Average Number of Trees (ha^{-1})
(a) Ambaro-Ambanja Bays (AAB)							
Closed-canopy mangrove	CC	Intact, tall, mature stands	<i>A. marina</i>	1	8.6	14.9	1250
			<i>C. tagal</i>	3	7.3 (\pm 1.2)	10.1 (\pm 0.5)	2625 (\pm 318)
			<i>R. mucronata</i>	14	7.0 (\pm 1.3)	10.1 (\pm 3.0)	4719 (\pm 1133)
			<i>S. alba</i>	1	5.6	10.6	5300
			Mixed species	2	6.7 (\pm 1.6)	11.3 (\pm 2.5)	1825 (\pm 248)
Open-canopy mangrove I	OC I	Medium stands	<i>R. mucronata</i>	2	4.8 (\pm 0.1)	9.5 (\pm 2.0)	1800 (\pm 141)
			Mixed species	2	4.8 (\pm 0.1)	9.5 (\pm 2.0)	1800 (\pm 141)
		Naturally open/very degraded tall very dense short stands	<i>Mixed species</i>	4	5.7 (\pm 0.3)	10.1 (\pm 1.2)	1525 (\pm 35)
			<i>C. tagal</i>	5	2.5 (\pm 0.3)	5.1 (\pm 0.9)	2780 (\pm 750)
			<i>R. mucronata</i>	2	4.8 (\pm 0.1)	7.8 (\pm 1.1)	5600 (\pm 1838)
Open-canopy mangrove II	OC II	Stunted, scrub ecosystems	<i>A. marina</i>	4	1.7 (\pm 0.5)	4.6 (\pm 0.2)	1306 (\pm 554)
(b) Mahajamba Bay (MHJ)							
Closed-canopy mangrove I	CC I	Tall, mature stands; canopy >80% closed	<i>A. marina</i>	7	10.24 (\pm 0.52)	13.68 (\pm 1.01)	1571 (\pm 255)
			<i>R. mucronata</i>	2	5.62 (\pm 0.55)	7.27 (\pm 1.69)	4900 (\pm 1500)
			<i>S. alba</i>	1	9.39	8.31	5100
			Mixed species	3	12.48 (\pm 1.40)	18.18 (\pm 1.56)	1108 (\pm 208)
Closed-canopy mangrove II	CC II	Tall mature stands; canopy >60% closed	<i>A. marina</i>	10	7.68 (\pm 0.56)	12.95 (\pm 1.26)	895 (\pm 102)
			Mixed species	2	7.74 (\pm 0.04)	12.45 (\pm 0.08)	1412 (\pm 12)
Open-canopy mangrove I	OC I	Short-medium stands; canopy 30%–70% closed; moderately influenced by background soil/mud	<i>A. marina</i>	6	3.32 (\pm 0.16)	4.85 (\pm 0.43)	1417 (\pm 226)
			<i>R. mucronata</i>	1	3.21	7.39	2200
			<i>X. granatum</i>	1	5.41	10.84	1300
			Mixed species	5	4.33 (\pm 0.44)	7.62 (\pm 0.86)	1185 (\pm 237)
Open-canopy mangrove II	OC II	Short-medium stands; canopy 30%–70% closed; significantly influenced by background soil/mud	<i>C. tagal</i>	2	3.39 (\pm 0.18)	6.18 (\pm 0.12)	963 (\pm 238)
			<i>R. mucronata</i>	4	4.63 (\pm 0.30)	7.85 (\pm 1.66)	1388 (\pm 449)
Open-canopy mangrove III	OC III	Stunted, short stands, very sparse; canopy < 30% closed; dominated by exposed soil/mud	<i>A. marina</i>	7	2.31 (\pm 0.17)	3.96 (\pm 0.18)	1089 (\pm 134)

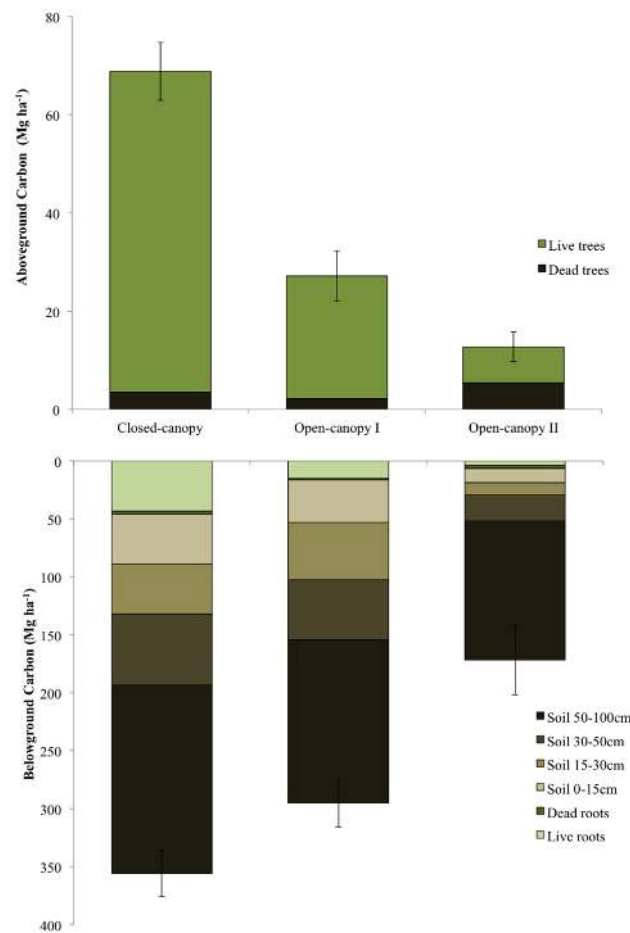


Figure 10. Total vegetation carbon and soil organic carbon stocks for the Ambaro-Ambanja Bays, Northwest Madagascar. Error bars represent \pm SE of total carbon stocks. Adapted from Jones *et al.* [62] with permission of Springer).

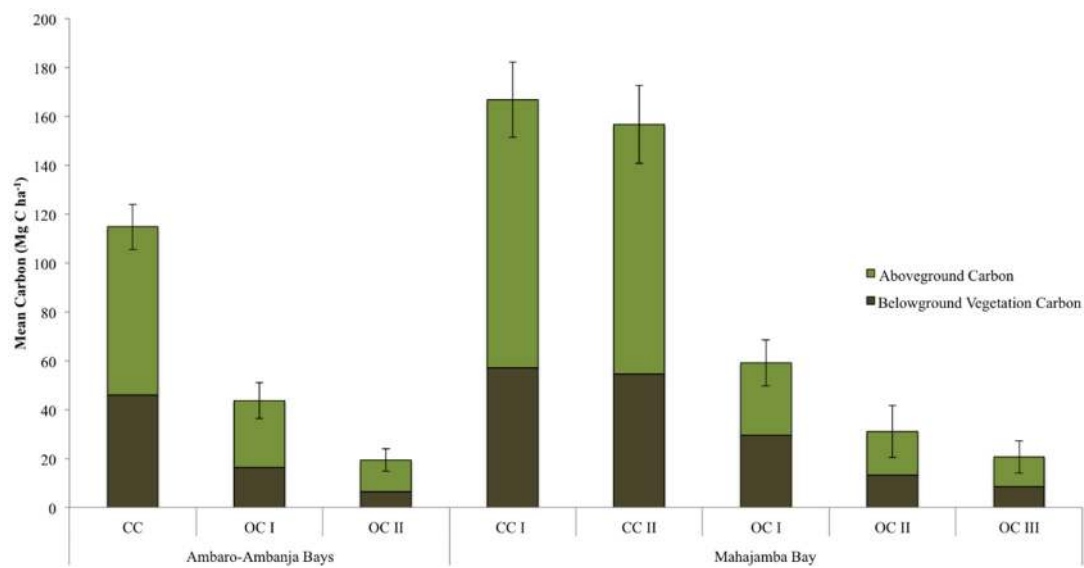


Figure 11. Above- and below-ground mangrove vegetation carbon estimates for the Ambaro-Ambanja Bays (AAB) [62] and Mahajamba Bay (MHJ) [61], Madagascar. Error bars represent \pm SE of total vegetation carbon stocks. Adapted from Jones *et al.* [61].

Mapping and modelling of historical ecosystem loss is a critical element in both the assessment of feasibility and the development of carbon projects. The generation of carbon credits through the conservation, restoration and reduced-impact use of mangroves has the potential to catalyze and fund sustainable mangrove management in coastal communities, augmenting existing livelihoods, preparing for climate change and safeguarding biodiversity. While national-level datasets are very valuable for the initial selection of potential project sites, the limitations outlined in Section 3.3.1 prevent them from being suitable for ecosystem-specific/project-scale historical deforestation analysis in Madagascar. The existing (*i.e.*, AAB and MHJ) and new (*i.e.*, TMD and BdA) AOI-specific maps presented in here can be used as a starting point for more detailed project-scale deforestation analysis, and also as a baseline for future project monitoring.

Working with local communities, the University of Antananarivo and other partners in AAB, the Blue Forests programme is using the data described above to assess the feasibility of a community-centered mangrove carbon project validated under the VCS standard (www.v-c-s.org), which focusses on the locally-led conservation and sustainable use of AAB's mangrove resources.

In TMD, in addition to supporting WWF Madagascar West Indian Ocean Programme Office's broader work in the region, the mapping detailed herein was also central to assessing the feasibility of a mangrove carbon project in the region].

In BdA, Blue Ventures is supporting communities to develop a Plan Vivo mangrove carbon project. Plan Vivo initiatives differ from other types of forest carbon projects. Whilst they are still measured and valued according to their impact on greenhouse gas emissions, Plan Vivo project design must be community-led. Fifty-two Plan Vivo projects have been initiated throughout the world to date, yet in only three countries (*i.e.*, Kenya, Columbia and Madagascar) are there projects focusing specifically on mangroves.

By piloting and developing mangrove carbon projects in close contact with in-country government institutions, the Blue Forests programme is supplying robust greenhouse gas emissions reductions estimates and helping to integrate mangroves into Madagascar's national REDD+ strategy.

4. Conclusions

This study presents, for the first time, national-level and mangrove ecosystem specific dynamics for Madagascar from 1990 to 2010, providing an unprecedented overview of mangrove loss. While not without their limitations, our AOI-specific contemporary maps offer numerous improvements over national-level USGS data-sets, providing detailed and accurate coverage of spectrally and ecologically distinct mangrove types and surrounding land-cover categories for two new specific Madagascan mangrove ecosystems (*i.e.*, TMD and BdA); building on and complementing similar maps for AAB and MHJ. Taken as a whole, these maps are the first of their kind for AAB and TMD, and provide updated information and improved thematic detail for MHJ and BdA. The methods used are easily replicable and employ freely available Landsat data. Factoring in their strengths, the primary weakness of our AOI-specific maps is their inability to represent degradation. The ability to accurately detect degradation would be greatly augmented through the incorporation of complementary remotely sensed data-sets (e.g., LiDAR; radar; finer spatial resolution optical imagery) in further mapping and monitoring.

A continuation and acceleration of modification and deforestation of Madagascar's mangrove ecosystems will jeopardize if not halt key ecosystem services. The extent and consequences of the ripple effects from continued loss and degradation in to surrounding ecosystems is unknown. To help safeguard the long-term status of Madagascar's mangrove forests, improved resource management is required. The AOI-specific maps described in this study are being applied through Blue Ventures' Blue Forests programme towards standardizing replicable methods for improved, community-led mangrove resource management throughout Madagascar's mangroves and beyond. Resulting carbon stock estimates for AAB and MHJ include the first total (*i.e.*, above- and below-ground including soil) estimates published for Madagascar (*i.e.*, [25]), and the first total-tree estimates published for MHJ

(i.e., [61]). While carbon stock estimates for MHJ are limited to trees, they are still high, consistent with regional estimates, and highlight the importance of this ecosystem towards climate change mitigation. Ongoing soil analysis will also finalize SOC values for AAB and MHJ, and total carbon stock estimates for MHJ, TMD and BdA, resulting in comprehensive carbon stock estimates for all four AOIs.

AOI-specific maps are directly helping to explore the feasibility of mangrove carbon projects in AAB and TMD and support the establishment of a Plan Vivo project in BdA. In addition to carbon projects, the results presented in this study provide an invaluable updated scientific baseline for policy makers and civil society to identify efficient mangrove conservation strategies at the ecosystem or national scale.

Acknowledgments: This research was funded by the Global Environmental Facility’s Blue Forest project and grants from the Western Indian Ocean Marine Science Association, the John D. and Catherine T. MacArthur Foundation and the Darwin Initiative. All TMD analysis was done in collaboration with the World Wildlife Fund’s Madagascar West Indian Ocean Programme Office. The authors greatly appreciate the logistical support for field work in MHJ provided by AQUALMA. Many thanks to Raymond Raheirindray, Zo Andriamahenina, Ismael Ratefinjanahary, Jaona Ravelonjatovo, Ferdinand Botsy, Tina Haingonirina and Holy Andriamitantsoa for assisting with field missions. Thanks also to Kate England, Bienvenue Zafindrasilivonona, Sylvia Paulot, Pierre-Francois Roy and Rado Rakotomanana for contributions to socio-economic research and analysis. Special thanks to community members from within all AOIs for their guidance, hospitality and assistance with field work. Additional thanks to extremely helpful anonymous reviewers.

Author Contributions: Trevor Jones took the lead on designing and undertaking the dynamics assessment, AOI-specific mapping, and writing the manuscript. Leah Glass assisted with the dynamics assessment and AOI-specific mapping and helped provide oversight for the manuscript, contextualizing loss. Samir Gandhi assisted with geospatial data pre-processing, the dynamics assessment, AOI-specific mapping and formatting the manuscript. Lalao Ravaoarinosihoarana helped design, and lead field missions, summarize resulting data, and further helped with carbon stock estimates. Aude Carro provided specific input regarding contextualizing mangrove loss. Lisa Benson assisted with calculating, compiling and presenting carbon stock estimates. Harifidy Rakoto Ratsimba helped design and provided oversight of field missions, and assisted with the dynamics assessment and AOI-specific mapping. Chandra Giri assisted with the dynamics assessment and AOI-specific mapping. Dannick Randriamanatena assisted with all logistics, field work and mapping related to TMD. Garth Cripps helped provide overall oversight on design and implementation.

Conflicts of Interest: The authors declare no conflict of interest.

References

1. Lugo, A.E.; Snedaker, S.C. The ecology of mangroves. *Annu. Rev. Ecol. Syst.* **1974**, *5*, 39–64. [[CrossRef](#)]
2. Blasco, F.; Bellan, M.F.; Chaudhury, M.U. Estimating the extent of floods in Bangladesh—Using SPOT data. *Remote Sens. Environ.* **1992**, *39*, 167–178. [[CrossRef](#)]
3. Marshall, N. Mangrove conservation in relation to overall environmental considerations. *Hydrobiologia* **1994**, *285*, 303–309. [[CrossRef](#)]
4. Primavera, J.H. Socio-economic impacts of shrimp culture. *Aquac. Res.* **1997**, *28*, 815–827. [[CrossRef](#)]
5. Kathiresan, K.; Bingham, B. Biology of mangroves and mangrove ecosystems. *Adv. Mar. Biol.* **2001**, *40*, 81–251.
6. Alongi, D.M. Present state and future of world’s mangrove forest. *Environ. Conserv.* **2002**, *29*, 331–349. [[CrossRef](#)]
7. Mumby, P.J.; Edwards, A.J.; Arias-González, E.; Lindeman, K.C.; Blackwell, P.G.; Gall, A.; Gorczyńska, M.I.; Harborne, A.R.; Pescod, C.L.; Renken, H.; *et al.* Mangrove enhance the biomass of coral reef fish communities in the Caribbean. *Nature* **2004**, *427*, 533–536. [[CrossRef](#)] [[PubMed](#)]
8. Dahdouh-Guebas, F.; Jayatissa, L.P.; di Nitto, D.; Bosire, J.O.; Lo Seen, D.; Koedam, N. How effective were mangroves as a defence against the recent tsunami? *Curr. Biol.* **2005**, *15*, R443–R447. [[CrossRef](#)] [[PubMed](#)]
9. Barbier, E.B. Natural barriers to natural disasters: Replanting mangroves after tsunami. *Front. Ecol. Environ.* **2006**, *4*, 124–131. [[CrossRef](#)]
10. Food and Agricultural Organization (FAO). *The World’s Mangroves 1980–2005*; FAO Forestry Paper 153; FAO: Rome, Italy, 2007.
11. Alongi, D.M. Mangrove forests: Resilience, protection from tsunamis, and responses to global climate change. *Estuar. Coast. Shelf Sci.* **2008**, *76*, 1–13. [[CrossRef](#)]

12. Nagelkerken, I.; Blaber, S.J.; Bouillon, S.; Green, P.; Haywood, M.; Kirton, L.G.; Meynecke, J.-O.; Pawlik, J.; Penrose, H.M.; Sasekumar, A.; *et al.* The habit function of mangroves for terrestrial and marine fauna: A review. *Aquat. Bot.* **2008**, *89*, 155–185. [[CrossRef](#)]
13. Alongi, D.M. Carbon payments for mangrove conservation: Ecosystem constraints and uncertainties of sequestration potential. *Environ. Sci. Policy* **2011**, *14*, 462–470. [[CrossRef](#)]
14. Donato, D.C.; Kauffman, J.B.; Murdiyarsa, D.; Kumianto, S.; Stidham, M.; Kanninen, M. Mangroves among the most carbon-rich forests in the tropics. *Nat. Geosci.* **2011**, *4*, 293–297. [[CrossRef](#)]
15. Kueznar, C.; Bluemel, A.; Gebhardt, S.; Quoc, T.V.; Dech, S. Remote sensing of mangrove ecosystems: A review. *Remote Sens.* **2011**, *3*, 878–928.
16. Pendleton, L.; Donato, D.C.; Murray, B.C.; Crooks, S.; Jenkins, W.A.; Sifleet, S.; Craft, C.; Fourqurean, J.W.; Kauffman, J.B.; Marba, N.; *et al.* Estimating global “blue carbon” emissions from conversion and degradation of vegetated coastal ecosystems. *PLoS ONE* **2012**, *7*, e43542. [[CrossRef](#)] [[PubMed](#)]
17. Kauffman, J.B.; Heider, C.; Norfolk, J.; Payton, F. Carbon stocks of intact mangroves and carbon emissions arising from their conversion in the Dominican Republic. *Ecol. Appl.* **2014**, *24*, 518–527. [[CrossRef](#)] [[PubMed](#)]
18. Thompson, B.S.; Clubbe, C.P.; Primavera, J.H.; Curnick, D.; Koldeway, H.J. Locally assessing the economic viability of blue carbon: A case study from Panay Island, the Philippines. *Ecosyst. Serv.* **2014**, *8*, 128–140. [[CrossRef](#)]
19. Giri, C.; Long, J.; Abbas, S.; Mani Murali, R.; Qamer, F.M.; Pengra, B.; Thau, D. Distribution and dynamics of mangrove forests of South Asia. *J. Environ. Manag.* **2015**, *148*, 101–111. [[CrossRef](#)] [[PubMed](#)]
20. Huxham, M.; Emerton, L.; Kairo, J.; Munyi, F.; Abdirizak, H.; Muriuki, T.; Nunan, F.; Briers, R.A. Applying Climate Compatible Development and economic valuation to coastal management: A case study of Kenya’s mangrove forests. *J. Environ. Manag.* **2015**, *157*, 168–181. [[CrossRef](#)] [[PubMed](#)]
21. Kauffman, J.B.; Heider, C.; Cole, T.G.; Dwire, K.A.; Donato, D.C. Ecosystem carbon stocks of Micronesian mangrove forests. *Wetlands* **2011**, *31*, 343–352. [[CrossRef](#)]
22. Adame, M.F.; Kauffman, J.B.; Medina, I.; Gamboa, J.N.; Torres, O.; Caamal, J.P.; Reza, M.; Herrera-Silveira, J.A. Carbon stocks of tropical coastal wetlands within the Karstic landscape of the Mexican Caribbean. *PLoS ONE* **2013**, *8*, e56569. [[CrossRef](#)] [[PubMed](#)]
23. Wang, G.; Dongsheng, G.; Peart, M.R.; Chen, Y.; Peng, Y. Ecosystem carbon stocks of mangrove forest in Yingluo Bay, Guangdong Province of South China. *For. Ecol. Manag.* **2013**, *310*, 539–546. [[CrossRef](#)]
24. Kauffman, J.B.; Donato, D.C. *Protocols for the Measurement, Monitoring and Reporting of Structure, Biomass and Carbon Stocks in Mangrove Forests*; Working Paper 86; CIFOR: Bogor, Indonesia, 2012.
25. Jones, T.G.; Ratsimba, H.R.; Ravaoarinorotsihoarana, L.; Cripps, G.; Bey, A. Ecological Variability and Carbon Stock Estimates of Mangrove Ecosystems in Northwestern Madagascar. *Forests* **2014**, *5*, 177–205. [[CrossRef](#)]
26. Valiela, I.; Bowen, J.L.; York, J.K. Mangrove forests: One of the world’s threatened major tropical environments. *Bioscience* **2001**, *51*, 807–815. [[CrossRef](#)]
27. Duke, N.C.; Meynecke, J.O.; Dittmann, S.; Ellison, A.M.; Anger, K.; Berger, U.; Cannicci, S.; Diele, K.; Ewel, K.C.; Field, C.D.; *et al.* A world without mangroves? *Science* **2007**, *317*, 41–42. [[CrossRef](#)] [[PubMed](#)]
28. Spalding, M.; Kainuma, M.; Collins, L. *World Atlas of Mangroves*; Earthscan: London, UK, 2010.
29. Friess, D.A.; Webb, E.L. Variability in mangrove change estimates and implications for the assessment of ecosystem provision. *Glob. Ecol. Biogeogr.* **2013**, *23*, 715–725. [[CrossRef](#)]
30. Alongi, D.M. The Impact of Climate Change on Mangrove Forests. *Curr. Clim. Chang. Rep.* **2015**, *1*, 30–39. [[CrossRef](#)]
31. Farnsworth, E.J.; Ellison, A.M. The global conservation status of mangroves. *Ambio* **1997**, *26*, 328–334.
32. Primavera, J.H. Development and conservation of Philippine mangroves: Institutional issues. *Ecol. Econ.* **2000**, *35*, 91–106. [[CrossRef](#)]
33. Dahdouh-Guebas, F. The use of remote sensing and GIS in the sustainable management of tropical coastal ecosystems. *Environ. Dev. Sustain.* **2002**, *4*, 93–112. [[CrossRef](#)]
34. Primavera, J.H. Mangroves, fishponds, and the quest for sustainability. *Science* **2005**, *310*, 57–59. [[CrossRef](#)] [[PubMed](#)]
35. Gopal, B.; Chauhan, M. Biodiversity and its conservation in the Sundarban Mangrove Ecosystem. *Aquat. Sci.* **2006**, *68*, 338–354. [[CrossRef](#)]
36. Primavera, J.H. Overcoming the impacts of aquaculture on the coastal zone. *Ocean Coast. Manag.* **2006**, *49*, 531–545. [[CrossRef](#)]

37. Gilman, E.L.; Ellison, J.; Duke, N.C.; Field, C. Threats to mangroves from climate change and adaptation options: A review. *Aquat. Bot.* **2008**, *89*, 237–250. [[CrossRef](#)]
38. Walters, B.B.; Rönnbäck, P.; Kovacs, J.M.; Crona, B.; Hussain, S.A.; Badola, R.; Primavera, J.H.; Barbier, E.; Dahdouh-Guebas, F. Ethnobiology, socio-economics and management of mangrove forests: A review. *Aquat. Bot.* **2008**, *89*, 220–236. [[CrossRef](#)]
39. Webb, E.L.; Jachowski, N.R.A.; Phelps, J.; Friess, D.A.; Than, M.M.; Ziegler, A.D. Deforestation in the Ayeyarwady Delta and the conservation implications of an internationally-engaged Myanmar. *Glob. Environ. Chang.* **2014**, *24*, 321–333. [[CrossRef](#)]
40. Siteo, A.A.; Mandlate, L.J.C.; Guedes, B.S. Biomass and Carbon Stocks of Sofala Bay Mangrove Forests. *Forests* **2014**, *5*, 1967–1981. [[CrossRef](#)]
41. Field, C.D. Impact of expected climate change on mangroves. *Hydrobiologia* **1995**, *295*, 75–81. [[CrossRef](#)]
42. Krauss, K.W.; Lovelock, C.E.; McKee, K.L.; Lopez-Hoffman, L.; Ewe, S.M.L.; Sousa, W.P. Environmental drivers in mangrove establishment and early development: A review. *Aquat. Bot.* **2008**, *89*, 105–127. [[CrossRef](#)]
43. Chan, H.T.; Baba, S. *Manual on Guidelines for Rehabilitation of Coastal Forests Damaged by Natural Hazards in the Asia-Pacific Region*; International Society for Mangrove Ecosystems (ISME) and International Tropical Timber Organization (ITTO): Okinawa, Japan, 2009; p. 66.
44. Suzuki, T.; Zijlema, M.; Burger, B.; Meijer, M.C.; Narayan, S. Wave dissipation by vegetation with layer schematization in SWAN. *Coast. Eng.* **2012**, *59*, 64–71. [[CrossRef](#)]
45. Di Nitto, D.; Neukermans, G.; Koedman, N.; Defever, H.; Pattyn, F.; Kairo, J.G.; Dahdouh-Guebas, F. Mangroves facing climate change: Landward migration potential in response to projected scenarios of sea level rise. *Biogeosciences* **2014**, *11*, 857–871. [[CrossRef](#)]
46. Polidoro, B.A.; Carpenter, K.E.; Collins, L.; Duke, N.C.; Ellison, A.M.; Ellison, J.C.; Farnsworth, E.J.; Fernando, E.S.; Kathiresan, K.; Koedam, N.E.; *et al.* Mangrove extinction risk and geographic areas of global concern. *PLoS ONE* **2010**, *5*, e10095. [[CrossRef](#)] [[PubMed](#)]
47. Daru, B.H.; Yessoufou, K.; Mankga, L.T.; Davies, J. A Global Trend towards the Loss of Evolutionarily Unique Species in Mangrove Ecosystems. *PLoS ONE* **2013**, *8*, 1–9. [[CrossRef](#)] [[PubMed](#)]
48. Heumann, B.W. Satellite remote sensing of mangrove forests: Recent advances and future opportunities. *Prog. Phys. Geogr.* **2011**, *35*, 87–108. [[CrossRef](#)]
49. Manson, F.J.; Loneragan, N.R.; McLeod, I.M.; Kenyon, R.A. Assessing techniques for estimating the extent of mangroves: Topographic maps, aerial photographs, and Landsat TM images. *Mar. Freshw. Res.* **2001**, *52*, 787–792. [[CrossRef](#)]
50. Ruiz-Luna, A.; Berlanga-Robles, C.A. Land use, land cover changes and coastal lagoon surface reduction associated with urban growth in northwest Mexico. *Landsc. Ecol.* **2003**, *18*, 159–171. [[CrossRef](#)]
51. Cornejo, R.H.; Koedam, N.; Luna, A.R.; Troell, M.; Dahdouh-Guebas, F. Remote sensing and ethno-botanical assessment of the mangrove forest changes in the Navachiste-San Ignacio-Macapule lagoon complex, Sinaloa, Mexico. *Ecol. Soc.* **2005**, *10*, 16.
52. Beland, M.; Goita, K.; Bonn, F.; Pham, T.T.H. Assessment of land-cover changes related to shrimp aquaculture using remote sensing data: A case study in the Giao Thuy District, Vietnam. *Int. J. Remote Sens.* **2006**, *27*, 1491–1510. [[CrossRef](#)]
53. Giri, C.; Pengra, B.; Zhu, Z.L.; Singh, A.; Tieszen, L.L. Monitoring mangrove forest dynamics of the Sundarbans in Bangladesh and India using multi-temporal satellite data from 1973 to 2000. *Estuar. Coast. Shelf Sci.* **2007**, *73*, 91–100. [[CrossRef](#)]
54. Giri, C.; Zhu, Z.; Tieszen, L.L.; Singh, A.; Gillette, S.; Kelmelis, J.A. Mangrove forest distributions and dynamics (1975–2005) of the tsunami-affected region of Asia. *J. Biogeogr.* **2008**, *35*, 519–528. [[CrossRef](#)]
55. Liu, K.; Li, X.; Shi, X.; Wang, S.G. Monitoring mangrove forest changes using remote sensing and GIS data with decision-tree learning. *Wetlands* **2008**, *28*, 336–346. [[CrossRef](#)]
56. Paling, E.I.; Kobryn, H.T.; Humphreys, G. Assessing the extent of mangrove change caused by Cyclone Vance in the eastern Exmouth Gulf, northwestern Australia. *Estuar. Coast. Shelf Sci.* **2008**, *77*, 603–613. [[CrossRef](#)]
57. Giri, C.; Ochieng, E.; Tieszen, L.L.; Zhu, Z.; Singh, A.; Loveland, T.; Masek, J.; Duke, N. Status and distribution of mangrove forests of the world using earth observation satellite data. *Glob. Ecol. Biogeogr.* **2011**, *20*, 154–159. [[CrossRef](#)]

58. Alsaadeh, B.; Al-Hanbali, A.; Tateishi, R.; KoBayashi, T.; Hoan, N.T. Mangrove forests mapping in the southern part of Japan using Landsat ETM+ with DEM. *J. Geogr. Inf. Syst.* **2013**, *5*, 369–377. [[CrossRef](#)]
59. Li, M.S.; Mao, L.J.; Shen, W.J.; Liu, S.Q.; Wei, A.I. Change and fragmentation trends of Zhanjiang mangrove forests in southern China using multi-temporal Landsat imagery (1977–2010). *Estuar. Coast. Shelf Sci.* **2013**, *130*, 111–120. [[CrossRef](#)]
60. Nguyen, H.; McAlpine, C.; Pullar, D.; Johansen, K.; Duke, N. The relationship of spatial-temporal changes in fringe mangrove extent and adjacent land-use: Case study of Ken Giang coast, Vietnam. *Ocean Coast. Manag.* **2013**, *76*, 12–22. [[CrossRef](#)]
61. Jones, T.G.; Ratsimba, H.R.; Ravaoarinorotsihoarana, L.; Glass, L.; Benson, L.; Teoh, M.; Carro, A.; Cripps, G.; Giri, C.; Gandhi, S.; *et al.* The Dynamics, Ecological Variability and Estimated Carbon Stocks of Mangroves in Mahajamba Bay, Madagascar. *J. Mar. Sci. Eng.* **2015**, *3*, 793–820. [[CrossRef](#)]
62. Jones, T.G.; Ratsimba, H.R.; Carro, A.; Ravaoarinorotsihoarana, L.; Glass, L.; Teoh, M.; Benson, L.; Cripps, G.; Giri, C.; Zafindrasilivonona, B.; *et al.* The mangroves of Ambanja and Ambaro Bays, northwest Madagascar: Historical dynamics, current status and deforestation mitigation strategy. In *Estuaries: A Lifeline of Ecosystem Services in Western Indian Ocean*; Diop, S., Scheren, P., Eds.; Springer International Publishing: Cham, Switzerland, 2016; in press.
63. Giri, S.; Mukhopadhyay, A.; Hazra, S.; Mukherjee, S.; Roy, D.; Ghosh, S.; Ghosh, T.; Mitra, D. A study on abundance and distribution of mangrove species in Indian Sundarban using remote sensing technique. *J. Coast. Conserv.* **2014**, *18*, 359–367. [[CrossRef](#)]
64. Jhonnerie, R.; Siregar, V.P.; Nababan, B.; Prasetyo, L.B.; Wouthuyzen, S. Random Forest Classification for Mangrove Land Cover Mapping Using Landsat 5 TM and Alos Palsar Imageries. *Procedia Environ. Sci.* **2015**, *24*, 215–221. [[CrossRef](#)]
65. Ramdani, F.; Rahman, S.; Setiani, P. Inexpensive Method to Assess mangroves Forest through the Use of Open Source Software and Data Available Freely in Public Domain. *J. Geogr. Inf. Syst.* **2015**, *7*, 43–57. [[CrossRef](#)]
66. Moffett, K.B.; Nardin, W.; Silvestri, S.; Wang, C.; Temmerman, S. multiple stable states and catastrophic shifts in coastal wetlands: Progress, challenges, and opportunities in validating theory using remote sensing and other methods. *Remote Sens.* **2015**, *7*, 10184–10226. [[CrossRef](#)]
67. Nardin, W.; Locatelli, S.; Pasquarella, V.; Rulli, M.C.; Woodcock, C.E.; Fagherazzi, S. Dynamics of a fringe mangrove forest detected by Landsat images in the Mekong delta, Vietnam. *Earth Surf. Process. Landf.* **2015**, in press.
68. Giri, C.; Muhlhausen, J. Mangrove forest distributions and dynamics in Madagascar (1975–2005). *Sensors* **2008**, *8*, 2104–2117. [[CrossRef](#)]
69. Giri, C. *National-Level Mangrove Cover Data-Sets for 1990, 2000 and 2010*; United States Geological Survey: Sioux Falls, SD, USA, 2011.
70. Mayaux, P.; Gond, V.; Bartholome, E. A near-real time forest-cover map of Madagascar derived from SPOT-4 VEGETATION data. *Int. J. Remote Sens.* **2000**, *21*, 3139–3144. [[CrossRef](#)]
71. Critical Ecosystem Partnership Fund (CEPF). *Madagascar Vegetation Mapping Project*; CEPF: Arlington, VA, USA, 2007.
72. Harper, G.J.; Steininger, M.K.; Tucker, C.J.; Juhn, D.; Hawkins, F. Fifty years of deforestation and forest fragmentation in Madagascar. *Environ. Conserv.* **2007**, *34*, 325–333. [[CrossRef](#)]
73. Rasolofoharinoro, M.; Blasco, F.; Bellan, M.F.; Aizpuru, M.; Gauquelin, T.; Denis, J. A remote sensing based methodology for mangrove studies in Madagascar. *Int. J. Remote Sens.* **1998**, *19*, 1873–1886. [[CrossRef](#)]
74. Pasqualini, V.; Iltis, J.; Dessay, N.; Lointier, M.; Guelorget, O.; Polidori, L. Mangrove mapping in North-Western Madagascar using SPOT-XS and SIR-C radar data. *Hydrobiologia* **1999**, *413*, 127–133. [[CrossRef](#)]
75. Guillet, M.; Renou, E.; Robin, M.; Debaine, F.; Ratsivalaka, S. Suivi et analyse de l'évolution de la mangrove de Mahajamba (Nord-ouest de Madagascar). In Proceedings of the International Pluridisciplinary Conference, Lille, France, 16–18 January 2008.
76. Raharimahefa, T.; Kusky, T.M. Environmental monitoring of Bombetoka Bay and the Betsiboka Estuary, Madagascar, using multi-temporal satellite data. *J. Earth Sci.* **2010**, *21*, 210–226. [[CrossRef](#)]
77. Rakotomavo, A.; Fromard, F. Dynamics of mangrove forests in the Mangoky River delta, Madagascar, under the influence of natural and human factors. *For. Ecol. Manag.* **2010**, *259*, 1161–1169. [[CrossRef](#)]

78. Law No. 97–017 on the Revision of Forestry Legislation; Articles 2 & 41. Government of Madagascar (GoM): Antananarivo, Madagascar, 1997.
79. Inter-Ministerial Order No. 4355/97 on the Definition of the Sensitive Areas; Articles 2 & 3. Government of Madagascar (GoM): Antananarivo, Madagascar, 1997.
80. Decree No. 98–781 Defining The Conditions of Application of the National Forest Policy; Articles 34 & 35. Government of Madagascar (GoM): Antananarivo, Madagascar, 1998.
81. Prohibiting Any Extractive Activity of Wood Resources in Sensitive Areas; Order No. 12.704/2000 of 20 November, 2000. Government of Madagascar (GoM): Antananarivo, Madagascar, 2000.
82. Decree No. 2005–849 of 13 December 2005 Revising the General Conditions of Application of Law No. 97–017 of 8 August 1997, Revising Forestry Legislation; Government of Madagascar (GoM): Antananarivo, Madagascar, 2005; Chapter 4.
83. Law No. 2008–013 on the Public Domain, Government Gazette of 2008; Article 3(a). Government of Madagascar (GoM): Antananarivo, Madagascar, 2008.
84. Government of Madagascar (GoM). Order No. 2055–2009 Creating Biologically Sensitive Shrimp Zones in Zone A in Ambaro Bay; Government of Madagascar (GoM): Antananarivo, Madagascar, 2009.
85. Prohibiting Any Exploitation of Mangrove Wood on the National Territory; Inter-Ministerial Order No. 32.100/2014 of 24 October, 2014; Government of Madagascar (GoM): Antananarivo, Madagascar, 2014.
86. Jones, T.G. Shining a light on Madagascar’s mangroves. *Madag. Conserv. Dev.* **2013**, *8*, 4–6.
87. Hughes, R.H.; Hughes, J.S. Region 6: Madagascar. In *A Directory of African Wetlands*, 1st ed.; IUCN: Gland, Switzerland; Cambridge, UK; UNEP: Nairobi, Kenya; WCMC: Cambridge, UK, 1992; pp. 793–806.
88. Vences, M.; Andreone, F.; Glaw, F.; Raminosoa, N.; Randrianirina, J.E.; Vieites, D.R. Amphibians and reptiles of the Ankaratra Massif: Reproductive diversity, biogeography and conservation of a montane fauna in Madagascar. *Ital. J. Zool.* **2002**, *69*, 263–284. [[CrossRef](#)]
89. Rasofolo, M.V. Use of mangroves by traditional fishermen in Madagascar. *Mangroves Salt Marshes* **1997**, *1*, 243–253. [[CrossRef](#)]
90. Roy, R.; Purkis, S.; Dunn, S. *Mapping Velondriake: The Application of Bathymetric and Marine Habitat Mapping to Support Conservation Planning, Southwest Madagascar*; Blue Ventures Internal Report; Blue Ventures: London, UK, 2009.
91. Tomlinson, P.B. *The Botany of Mangroves*; Cambridge University Press: Melbourne, Australia, 1986.
92. Chavez, P.S. Image-based atmospheric corrections: Revisited and improved. *Photogramm. Eng. Remote Sens.* **1996**, *62*, 1025–1036.
93. Kirui, K.B.; Kairo, J.G.; Bosire, J.; Viergever, K.M.; Rudra, S.; Huxham, M.; Briers, R.A. Mapping of mangrove forest land cover change along the Kenya coastline using Landsat imagery. *Ocean Coast. Manag.* **2013**, *83*, 19–24. [[CrossRef](#)]
94. Simard, M.; Zhang, K.Q.; Rivera-Monroy, V.H.; Ross, M.S.; Ruiz, P.L.; Castaneda-Moya, E.; Twilley, R.R.; Rodriguez, E. Mapping height and biomass of mangrove forests in Everglades National Park with SRTM elevation data. *Photogramm. Eng. Remote Sens.* **2006**, *72*, 299–311. [[CrossRef](#)]
95. Fatoyinbo, T.E.; Simard, M.; Washington-Allen, R.A.; Shugart, H.H. Landscape-scale extent, height, biomass, and carbon estimation of Mozambique’s mangrove forests with Landsat ETM+ and Shuttle Radar Topography Mission elevation data. *J. Geophys. Res. Biogeosci.* **2008**, *113*. [[CrossRef](#)]
96. Simard, M.; Rivera-Monroy, V.H.; Mancera-Pineda, J.E.; Castaneda-Moya, E.; Twilley, R.R. A systematic method for 3D mapping of mangrove forests based on Shuttle Radar Topography Mission elevation data, ICESat/GLAS waveforms and field data: Application to Cienaga Grande de Santa Marta, Colombia. *Remote Sens. Environ.* **2008**, *112*, 2131–2144. [[CrossRef](#)]
97. Fatoyinbo, T.E.; Simard, M. Height and biomass of mangroves in Africa from ICESat/GLAS and SRTM. *Int. J. Remote Sens.* **2013**, *34*, 668–681. [[CrossRef](#)]
98. Aslan, A.; Rahman, A.F.; Warren, M.; Robeson, S.M.; Darusman, T. Combined use of active and passive remote sensing for mapping distribution and biomass of coastal mangroves. In *Proceeding of American Geophysical Union Fall Meeting, San Francisco, CA, USA, 15–19 December 2014*.
99. Sinclair, T.T.; Hoffer, R.M.; Schreiber, M.M. Reflectance and internal structure of leaves from several crops during a growing season. *Agron. J.* **1971**, *63*, 864–868. [[CrossRef](#)]
100. Elvidge, C.D. Visible and near-infrared reflectance characteristics of dry plant materials. *Int. J. Remote Sens.* **1990**, *11*, 1775–1795. [[CrossRef](#)]

101. Bhattarai, B.; Giri, C. Assessment of mangrove forests in the Pacific region using Landsat imagery. *J. Appl. Remote Sens.* **2011**, *5*, 053509. [[CrossRef](#)]
102. Long, J.B.; Giri, C. Mapping the Philippines' mangrove forests using Landsat imagery. *Sensors* **2011**, *11*, 2972–2981. [[CrossRef](#)] [[PubMed](#)]
103. Aschbacher, J.; Ofren, R.; Delsol, J.P.; Suselo, T.B.; Vibulsresth, S.; Charrupat, T. An integrated comparative approach to mangrove vegetation mapping using advanced remote sensing and GIS technologies: Preliminary results. *Hydrologica* **1995**, *295*, 285–295.
104. Gao, J.A. Hybrid method toward accurate mapping of mangroves in a marginal habitat from SPOT Multispectral data. *Int. J. Remote Sens.* **1998**, *19*, 1887–1899. [[CrossRef](#)]
105. Green, E.P.; Clark, C.D.; Mumby, P.J.; Edwards, A.J.; Ellis, A.C. Remote sensing techniques for mangrove mapping. *Int. J. Remote Sens.* **1998**, *19*, 935–956. [[CrossRef](#)]
106. Gao, J.A. Comparative study on spatial and spectral resolutions of satellite data in mapping mangrove forests. *Int. J. Remote Sens.* **1999**, *20*, 2823–2833. [[CrossRef](#)]
107. Saito, H.; Bellan, M.F.; Al-Habshi, A.; Aizpuru, M.; Blasco, F. Mangrove research and coastal ecosystem studies with SPOT-4 HRVIR and TERRA ASTER in Arabian Gulf. *Int. J. Remote Sens.* **2003**, *24*, 4073–4092. [[CrossRef](#)]
108. Tong, P.H.; Auda, Y.; Populus, J.; Aizpura, M.; Habshi, A.A.; Blasco, F. Assessment from space of mangroves evolution in the Mekong Delta, in relation to extensive shrimp farming. *Int. J. Remote Sens.* **2004**, *25*, 4795–4812. [[CrossRef](#)]
109. Jensen, L.S.; Mueller, T.; Tate, K.R.; Ross, D.J.; Magid, J.; Nielsen, N.E. Soil surface CO₂ flux as an index of soil respiration *in situ*: A comparison of two chamber methods. *Soil Biol. Biochem.* **1996**, *28*, 1297–1306. [[CrossRef](#)]
110. Comley, B.W.T.; McGuinness, K.A. Above- and below-ground biomass, and allometry, of four common northern Australian mangroves. *Aust. J. Bot.* **2005**, *53*, 431–436. [[CrossRef](#)]
111. Curran, P.J. Remote sensing of foliar chemistry. *Remote Sens. Environ.* **1989**, *30*, 271–278. [[CrossRef](#)]
112. Komiyama, A.; Pongpan, S.; Kato, S. Common allometric equations for estimate the tree weight of mangroves. *J. Trop. Ecol.* **2005**, *21*, 471–477. [[CrossRef](#)]
113. Schumacher, B. *Methods for the Determination of Total Organic Carbon (TOC) in Soils and Sediments*; Ecological Risk Assessment Support Center, Office of Research and Development, US Environmental Protection Agency: Washington, DC, USA, 2002.
114. De Vos, B.; Letterns, S.; Muys, B.; Deckers, J.A. Walkley-Black analysis of forest soil organic carbon: Recovery, limitations and uncertainty. *Soil Use Manag.* **2007**, *23*, 221–229. [[CrossRef](#)]
115. Meersmans, J.; van Wesemael, B.; van Molle, M. Determining soil organic carbon for agricultural soils: A comparison between the Walkley & Black and the dry combustion methods (North Belgium). *Soil Use Manag.* **2009**, *25*, 346–353.
116. Ray, R.; Ganguly, D.; Chowdhury, C.; Dey, M.; Das, S.; Dutta, M.K.; Mandal, S.K.; Majumder, N.; De, T.K.; Mukhopadhyay, S.K.; *et al.* Carbon sequestration and annual increase of carbon stock in a mangrove forest. *Atmos. Environ.* **2011**, *45*, 5016–5024. [[CrossRef](#)]
117. Chen, L.; Zeng, X.; Tam, N.F.Y.; Lu, W.; Luo, Z.; Du, X.; Wang, J. Comparing carbon sequestration and stand structure of monoculture and mixed mangrove plantations of *Sonneratia caseolaris* and *S. apetala* in Southern China. *For. Ecol. Manag.* **2012**, *284*, 222–229. [[CrossRef](#)]
118. Donato, D.C.; Kauffman, J.B.; Mackenzie, R.A.; Ainsworth, A.; Pflieger, A.Z. Whole-island carbon stocks in the tropical Pacific: Implications for mangrove conservation and upland restoration. *J. Environ. Manag.* **2012**, *97*, 89–96. [[CrossRef](#)] [[PubMed](#)]
119. Fujimoto, K.; Imaya, A.; Tabuchi, R.; Kuramoto, S.; Utsugi, H.; Murofushi, T. Belowground C storage of Micronesian mangrove forests. *Ecol. Res.* **1999**, *14*, 409–413. [[CrossRef](#)]
120. Jardine, S.L.; Siikamäki, J.V. A global predictive model of carbon in mangrove soils. *Environ. Res. Lett.* **2014**, *9*, 104013. [[CrossRef](#)]
121. Liu, H.; Ren, H.; Hui, D.; Wang, W.; Liao, B.; Cao, Q. Carbon stocks and potential carbon storage in the mangrove forests of China. *J. Environ. Manag.* **2014**, *133*, 86–93. [[CrossRef](#)] [[PubMed](#)]

